第二百八號

（昭和十六年五月發行）

抄　錄

翼幅上に不連續點を有する翼の特性

（特に切り缺きの影響に關聯して）

囑託　岡　本　哲　史

本報告は前に發表した航研報告第 113, 131 號の續報で主として理論的のものを纏めたものである．この中には既に航研彙報第 113, 142, 159, 170, 174 號に發表したものが含まれてゐる．三部より成り第一部は翼幅上に不連續點を有する翼の揚力分布を求める近似計算法と題し．切り缺き，下げ翼，胴體，發動機ナセル，補助翼を有する翼に適用し得る簡便なる計算法を作り，かなりの精度を以て揚力分布を計算し得る事を示した．第二部は切り離された翼の特性と題し，縱隙間を有する翼の特性を計算し，その特別な場合として切り缺き，下げ翼，胴體を有する翼の特性を近似的に計算した．この計算結果は實驗結果とよく合致した．第三部は切り缺きを有する翼の特性と題し，先づ翼の二次元流に於ける揚力曲線の傾きを檢討し次に矩形切り缺きを有する翼の特性を計算した．計算結果は實驗結果とよく合致した．

No. 208.

(Published May, 1941)

The Characteristics of the Aerofoil with Discontinuities along the Span, with Special Reference to the Effects of Cut-Out.

By

Tetusi OKAMOTO, *Kôgakusi.*

Research Associate of the Institute.

Abstract.

The present paper deals theoretically with the aerofoil with discontinuities along the span like the aerofoil with rectangular cut-out, flap or aileron. It consists of three parts. In the first part the approximate method of calculating the lift distribution of the aerofoil with discontinuities is obtained, and it is shown that the present method may conveniently be used in practice with satisfactory accuracy. In the second part the characteristics of the aerofoil with longitudinal slots are studied, and as the special cases the divided aerofoil and the aerofoil with cut-out are solved. The calculated results agree satisfactorily with the measured results. In the third part the characteristics of the aerofoil with rectangular cut-out are calculated, showning that the calculated results agree satisfactorily with the experimental results.

Part 1. Approximate Method of Determining the Lift Distribution of the Aerofoil with Discontinuities.

§1.1. *Introduction.*

For the case of the aerofoil with sudden changes in the wing section along the span, most of the usual methods of calculating the lift distribution needs the great efforts, and yet the accuracy of the results is considerably low compared with the cases such as the rectangular or tapered aerofoils. The sudden changes in the wing section along the span occur very often in practice, as seen in the aerofoils with flap, allerons, engine nacelle or fuselage, and so it is desirable in designing aeroplane to find a convenient method of the calculation for such cases.

§1.2. *Lift distribution of the aerofoil of infinite span with a discontinuity.*

The lift distribution of the aerofoil of infinite span with a discontinuity in the spanwise distribution of the geometrical angle of incidence has been studied by Betz and Petersohn (Reference 1), but the case in which the chord, the slope of the lift curve and the angle of incidence change discontinuously along the span has not been studied.

Suppose that a discontinuity occurs at the origin, as shown in Fig. 1, and the sections in the ranges of $y>0$ and $y<0$ have the circulations $\Gamma_1 = c_{l1} V t_1 \alpha_1$ and $\Gamma_2 = c_{l2} V t_2 \alpha_2$, respectively, in two-dimensional flow, where $c_l = \frac{1}{2}\partial C_{z\infty}/\partial\alpha$, t is the chord length, V the velocity and α the geometrical angle of incidence.

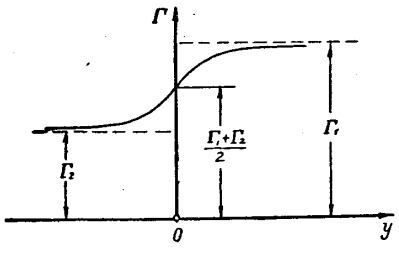

Fig. 1.

As the wing sections in the range of $y>0$ are in the velocity field induced by those in the range of $y<0$, the actual distribution of circulation may be seen to have such a form as shown in Fig. 1, in

which $\Gamma \to \Gamma_1$ when $y \to \infty$, $\Gamma \to \Gamma_2$ when $y \to -\infty$, and $\Gamma = \frac{1}{2}(\Gamma_1 + \Gamma_2)$ at the origin if Γ_2 is not too small compared with Γ_1.

Then, the distribution of circulation can be written in the form

$$\Gamma = \frac{\Gamma_1 + \Gamma_2 e^{-py}}{1 + e^{-py}}, \quad \cdots\cdots\cdots\cdots \quad (1)$$

where p is a positive number determination of which is our aim.

The induced velocity $w_{(y)}$ at any point on the span is calculated by the equation

$$w = \frac{1}{4\pi} \int_{-\infty}^{+\infty} \frac{\partial \Gamma}{\partial y'} \cdot \frac{dy'}{y - y'}$$

$$= \frac{P(\Gamma_1 - \Gamma_2)}{4\pi} \int_0^{\infty} \frac{e^{-py'}}{(1 + e^{-py'})^2} \cdot \frac{2y}{y^2 - y'^2} dy' \cdots\cdots \quad (2)$$

Putting $z = \frac{1}{2}(1 - e^{-py})$, then we get

$$\frac{e^{-py}}{(1 + e^{-py})^2} = \frac{e^{-py}}{4}(1 - z)^{-2} \fallingdotseq \frac{e^{-py}}{4}(2{\cdot}75 - 2{\cdot}5 e^{-py} + 0{\cdot}75 e^{-2py}),$$

$$\left.\begin{aligned} &\text{Hence} \qquad w = \frac{p(\Gamma_1 - \Gamma_2)}{4\pi} I_{(y)}, \\ &\text{where} \quad I_{(y)} = 0{\cdot}6875\, \Phi_1 - 0{\cdot}6250\, \Phi_2 + 0{\cdot}1875\, \Phi_3 \\ &\text{and} \qquad \Phi_n = e^{-npy} Ei(npy) - e^{npy} Ei(-npy), \quad (n = 1, 2, 3) \end{aligned}\right\} \quad (3)$$

$Ei(x)$ is the expotential integral whose numerical value can conveniently be obtained from the Table.(*)

When the angle of incidence is not so large, the relation between the effective angle of incidence α_e and the geometrical angle of incidence α is

$$\alpha_e = \alpha - \frac{w}{V} \cdots\cdots\cdots\cdots\cdots\cdots \quad (4)$$

(*) E. Janke and F. Emde; Funktionentafeln mit Formeln und Kurven.

Substituting the equation

$$\alpha_e = \frac{\Gamma_{\infty(y)}}{c_{1(y)} Vt_{(y)}} ,$$

where Γ_∞ is the circulation in two-dimensional flow, into the equation (4), then we get

$$\Gamma_{(y)} = c_{1(y)} Vt_{(y)} \alpha_{(y)} - c_{1(y)} t_{(y)} w_{(y)} \quad \cdots\cdots\cdots\cdots \quad (5)$$

This is the fundamental equation to determine the value of p. If we choose a suitable positive value of py, A say, and if we denote the corresponding point by y_1, then the equation (5) becomes

$$\frac{\Gamma_1 + \Gamma_2 e^{-A}}{1 + e^{-A}} = \Gamma_1 - \frac{c_{11} t_1}{4\pi} p(\Gamma_1 - \Gamma_2) I_{(y_1)} .$$

Hence,
$$p = \frac{4\pi k}{c_{11} t_1} ,$$

where
$$k = \frac{e^{-A}}{1 + e^{-A}} \cdot \frac{1}{I_{(y_1)}} \quad \cdots\cdots\cdots\cdots \quad (6)$$

If we take $A = 1{\cdot}5$(*), then we get

$$p = \frac{5{\cdot}27}{c_{11} t_1} \quad \cdots\cdots\cdots\cdots \quad (7)$$

The comparison of the circulation distribution obtained by the present method with that from Betz's method is shown in Fig. 2.

Rewriting the circulation distribution (1) in the same manner as Betz's method, we get

$$\Gamma = \frac{\Gamma_1 + \Gamma_2}{2} + \frac{\Gamma_1 - \Gamma_2}{2} \varepsilon ,$$

(*) The point of $py = 1{\cdot}5$ corresponds nearly to the point of the maximum induced velocity.

where $$\varepsilon = \tanh\frac{1}{2}py \quad \cdots\cdots\cdots\cdots\cdots\cdots \quad (8)$$

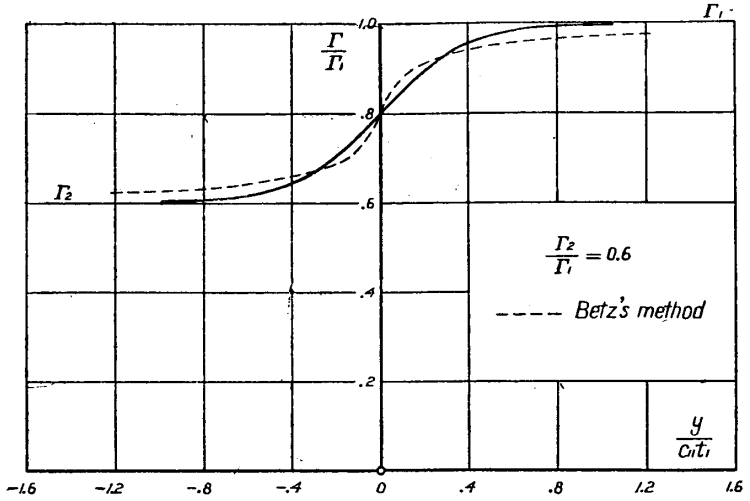

Fig. 2.

§1.3. *Lift distribution of the aerofoil of infinite span with two discontinuities.*

1.3.1. *Aerofoil with a nacelle or fuselage and aerofoil with rectangular cut-out.*

Suppose that the discontinuities occur at the points $y = \pm y_0$ and the sections in the ranges of $|y| > y_0$ and $|y| < y_0$ have the circulations $\Gamma_1 = c_{11}Vt_1\alpha_1$ and $\Gamma_2 = c_{12}Vt_2\alpha_2$, respectively, in two-dimensional flow, where we assume that $\Gamma_1 > \Gamma_2$ as shown in Fig. 3.

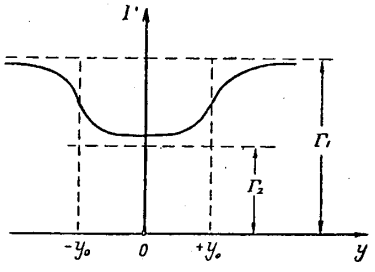

Fig. 3.

The circulation distribution can be written in the form

$$\Gamma = \frac{\Gamma_1 - \Gamma_2}{1 + e^{-p(y-y_0)}} + \frac{\Gamma_2 + \Gamma_1 e^{-p(y+y_0)}}{1 + e^{-p(y+y_0)}} \quad \cdots\cdots \quad (9)$$

The induced velocity at any point on the y-axis is

$$w = \frac{p(\Gamma_1-\Gamma_2)}{4\pi}\int_{-\infty}^{+\infty}\left[\frac{e^{-p(y'-y_0)}}{\{1+e^{-p(y'-y_0)}\}^2}-\frac{e^{-p(y'+y_0)}}{\{1+e^{-p(y'+y_0)}\}^2}\right]\frac{dy'}{y-y'}$$

$$= \frac{p(\Gamma_1-\Gamma_2)}{4\pi}\{\mathbf{I}_{(y-y_0)}-\mathbf{I}_{(y+y_0)}\}, \quad \cdots\cdots\cdots\cdots\cdots \quad (10)$$

where the integral $\mathbf{I}$ has shown by the equation (3) in §1.2.

If we denote the point corresponding to the suitably-chosen value of $p(y-y_0)$ by y_1, then the equation (5) becomes

$$\frac{\Gamma_1-\Gamma_2}{1+e^{-p(y_1-y_0)}}+\frac{\Gamma_2+\Gamma_1 e^{-p(y_1+y_0)}}{1+e^{-p(y_1+y_0)}} = \Gamma_1-\frac{c_{11}t_1}{4\pi}p(\Gamma_1-\Gamma_2)\{\mathbf{I}_{(y_1-y_0)}-\mathbf{I}_{(y_1+y_0)}\},$$

from which we get

$$\left.\begin{aligned} p &= \frac{4\pi k}{c_{11}t_1}, \\ \text{where} \quad k &= \frac{e^{-p(y_1-y_0)}-e^{-p(y_1+y_0)}}{1+e^{-p(y_1-y_0)}+e^{-p(y_1+y_0)}+e^{-2py_1}}\cdot\frac{1}{\mathbf{I}_{(y_1-y_0)}-\mathbf{I}_{(y_1+y_0)}} \end{aligned}\right\} \quad (11)$$

The values of $pc_{11}t_1$ calculated by taking $p(y_1-y_0)=1{\cdot}5$ in the similar manner as in the preceding article are shown as the function of $y_0/c_{11}t_1$ in Table 1 and Fig. 4.

TABLE 1.

$y_0/c_{11}t_1$	0	0·05	0·19	0·37	0·58	0·78	0·98	1·18	1·38	∞
$pc_{11}t_1$	∞	15·51	9·20	7·52	6·46	6·08	5·86	5·72	5·62	5·27

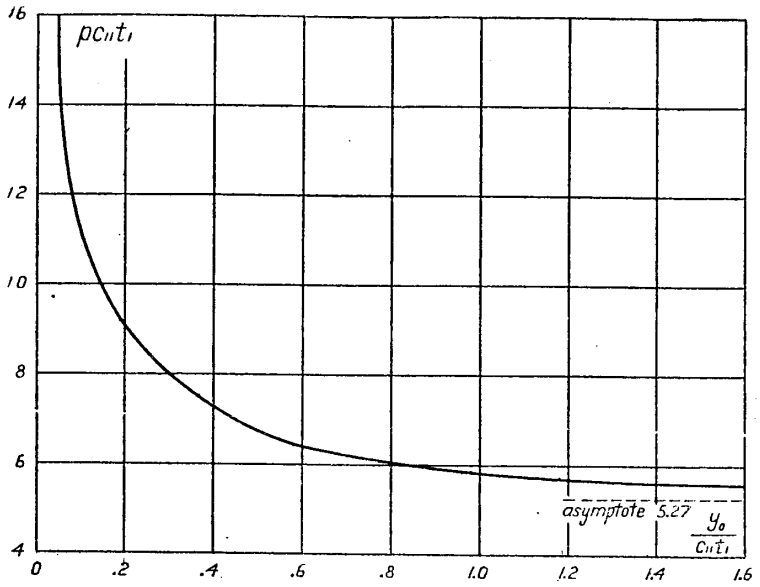

Fig. 4.

1.3.2. *Aerofoil with flap.*

Suppose that the discontinuities occur at the points $y = \pm y_0$ and the sections in the ranges of $-y_0 \leqq y \leqq y_0$ and $|y| > y_0$ have the circulations $\Gamma_2 = c_{12} V t_2 \alpha_2$ and $\Gamma_1 = c_{11} V t_1 \alpha_1$, respectively, in two-dimensional flow as shown in Fig. 5.

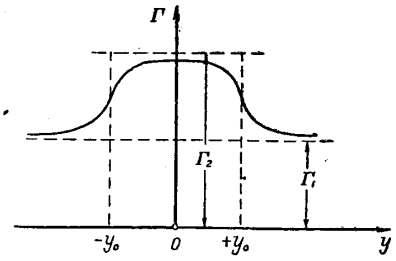

Fig. 5.

Then, the circulation distribution can be written in the form

$$\Gamma = \frac{\Gamma_1 + \Gamma_2 e^{-p(y-y_0)}}{1+e^{-p(y-y_0)}} + \frac{(\Gamma_1 - \Gamma_2) e^{-p(y+y_0)}}{1+e^{-p(y+y_0)}} \quad \cdots\cdots\cdots\cdots\cdots (12)$$

The induced velocity at any point on the y-axis is

$$w = \frac{p(\Gamma_2 - \Gamma_1)}{4\pi} \int_{-\infty}^{+\infty} \left[\frac{e^{-p(y'+y_0)}}{\{1+e^{-p(y'+y_0)}\}^2} - \frac{e^{-p(y'-y_0)}}{\{1+e^{-p(y'-y_0)}\}^2} \right] \frac{dy'}{y-y'}$$

$$= \frac{p(\Gamma_2 - \Gamma_1)}{4\pi} \{ I_{(y+y_0)} - I_{(y-y_0)} \} .$$

If we denote the point corresponding to the suitably-chosen value of $p(y-y_0)$ by y_1, then the equation (5) becomes

$$\frac{\Gamma_1+\Gamma_2 e^{-p(y_1-y_0)}}{1+e^{-p(y_1-y_0)}}+\frac{(\Gamma_1-\Gamma_2)e^{-p(y_1+y_0)}}{1+e^{-p(y_1+y_0)}} = \Gamma_1-\frac{c_{11}t_1}{4\pi}p(\Gamma_2-\Gamma_1)\{I_{(y_1+y_0)}-I_{(y_1-y_0)}\},$$

from which we get

$$\left.\begin{aligned} p &= \frac{4\pi k}{c_{11}t_1}, \\ \text{where}\quad k &= \frac{e^{-p(y_1+y_0)}-e^{-p(y_1-y_0)}}{1+e^{-p(y_1+y_0)}+e^{-p(y_1-y_0)}+e^{-2py_1}}\cdot\frac{1}{I_{(y_1+y_0)}-I_{(y_1-y_0)}} \end{aligned}\right\} \quad (13)$$

This equation is the same as the equation (11), and hence the values of p are the same as those shown in Table 1.

1.3.3. *Aerofoil with ailerons.*

Suppose that the discontinuities occur at the points $y=\pm y_0$ and the sections in the ranges of $y>y_0$, $y<-y_0$ and $-y_0\leqq y\leqq y_0$ have the circulations $\Gamma_1=c_{11}Vt_1\alpha_1$, $\Gamma_2=c_{12}Vt_2\alpha_2$ and $\Gamma_m=\frac{1}{2}(\Gamma_1+\Gamma_2)$, respectively, in two-dimensional flow, where we assume that $\Gamma_1>\Gamma_2$.

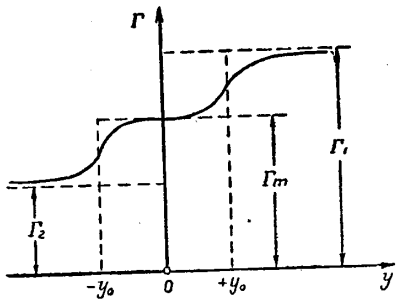

Fig 6.

Then, the circulation distribution can be written in the form

$$\Gamma=\frac{\Gamma_1+\Gamma_m e^{-p(y-y_0)}}{1+e^{-p(y-y_0)}}-\frac{(\Gamma_m-\Gamma_2)e^{-p(y+y_0)}}{1+e^{-p(y+y_0)}} \quad \cdots\cdots \quad (14)$$

The induced velocity at any point on the y-axis is

$$w=\frac{p(\Gamma_1-\Gamma_m)}{4\pi}\int_{-\infty}^{+\infty}\left[\frac{e^{-p(y'-y_0)}}{\{1+e^{-p(y'-y_0)}\}^2}+\frac{e^{-p(y'+y_0)}}{\{1+e^{-p(y'+y_0)}\}^2}\right]\frac{dy'}{y-y'}$$
$$=\frac{p(\Gamma_1-\Gamma_m)}{4\pi}\{I_{(y-y_0)}+I_{(y+y_0)}\}.$$

If we denote the point corresponding to the suitably-chosen value of $p(y-y_0)$ by y_1, then the equation (5) becomes

$$\frac{\Gamma_1+\Gamma_m e^{-(y_1-y_0)}}{1+e^{-y(y_1-y_0)}}-\frac{(\Gamma_1-\Gamma_m)e^{-p(y_1+y_0)}}{1+e^{-p(y_1+y_0)}}$$

$$=\Gamma_1-\frac{c_{11}t_1}{4\pi}p(\Gamma_1-\Gamma_m)\{I_{(y_1-y_0)}-I_{(y_1+y_0)}\},$$

from which we get

$$\left.\begin{aligned} &p=\frac{4\pi k}{c_{11}t_1},\\ \text{where}\quad &k=\frac{e^{-p(y_1-y_0)}+e^{-p(y_1+y_0)}+2e^{-2py_1}}{1+e^{-p(y_1-y_0)}+e^{-p(y_1+y_0)}+e^{-2py_1}}\cdot\frac{1}{I_{(y_1-y_0)}+I_{(y_1+y_0)}} \end{aligned}\right\}\quad(15)$$

The values of $pc_{11}t_1$ calculated by taking $p(y_1-y_0)=1{\cdot}5$ are shown as the function of $y_0/c_{11}t_1$ in Table 2 and Fig. 7.

TABLE 2.

$y_0/c_{11}t_1$	0	0·06	0·20	0·46	0·68	0·85	1·01	1·19	1·36	∞
$pc_{11}t_1$	5·27	4·40	3·79	3·77	4·07	4·44	4·68	4·85	4·95	5·27

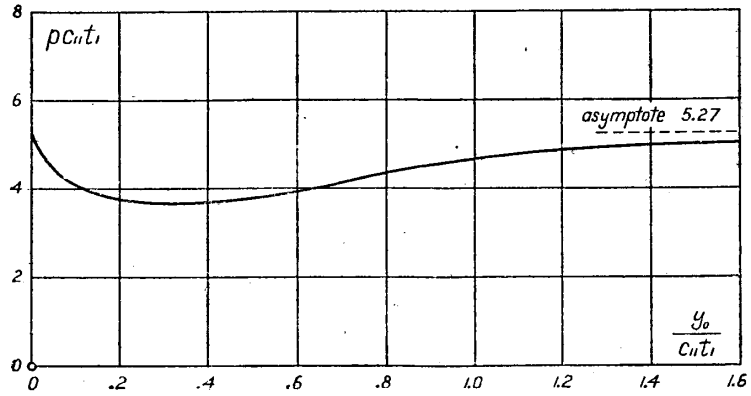

Fig. 7.

§1.4. *Lift distribution of the aerofoil of finite span with discontinuities.*

The above-mentioned method of calculation can be applied as it is for the aerofoil of finite span by placing Γ_1 and Γ_2 with the equations

$$\Gamma_1 = c_{11} V t_1 \alpha_1 \sum_0^\infty \sqrt{1-\eta^2} A_{1,n} \eta^{2n} \quad \text{and} \quad \Gamma_2 = c_{12} V t_2 \alpha_2 \sum_1^\infty \sqrt{1-\eta^2} A_{2,n} \eta^{2n},$$

according to Betz's method of representation, or

$$\Gamma_1 = c_{11} V t_1 \alpha_1 \sum_1^\infty A_{1,n} \sin n\theta \quad \text{and} \quad \Gamma_2 = c_{12} V t_2 \alpha_2 \sum_1^\infty A_{2,n} \sin n\theta,$$

according to Trefftz-Glauert's method of representation, where $\eta = y/b$, b = semi-span, and $y = -b\cos\theta$. Then, we can calculate the induced velocity and determine the value of p in the similar manner as in the preceding articles.

As the first approximation, however, we may use the values of p obtained in §1.2 and §1.3. Now, we compare the circulation distribution calculated by the present approximate method with that by Fourier-series

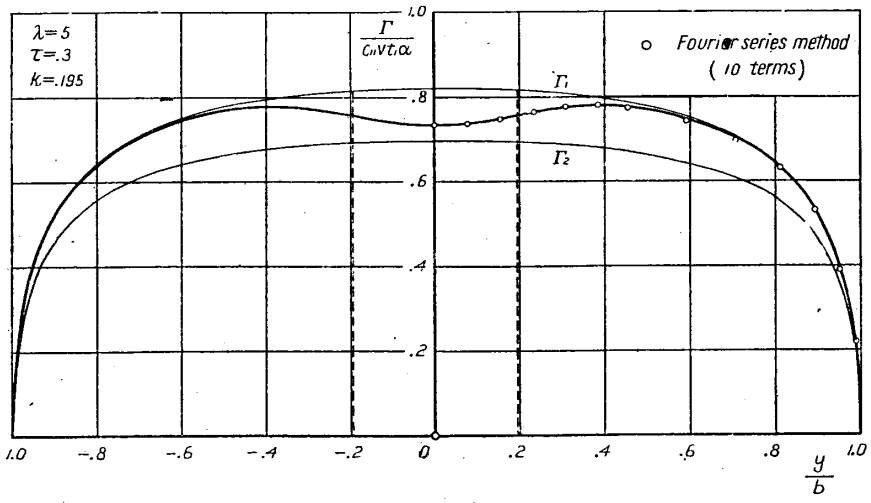

Fig. 8. Comparison of the circulation distribution calculated by the present method with that by Fouries-series method with respect to the aerofoil with cut-out.

method (see Part 3, §3.4) with respect to the aerofoil with cut-out of $\tau = 0{\cdot}3$ and $k = 0{\cdot}195$, where τ is the ratio of the depth of cut-out

to the chord length and k the ratio of the width of cut-out to the span. This comparison shows a good agreement as shown in Fig. 8. It is concluded that the present approximate method may conveniently be used in practice with satisfactory accuracy.

Part 2. Characteristics of Divided Aerofoil.

§2.1. *Aerofoil with the longitudinal slots.*

The characteristics of the aerofoil with two longitudinal slots can be determined by calculating the mutual interference between three divided portions. We assume that the end portions 1 and 3 have the same wing section and the central portion has a different wing section.

For the sake of simplicity we assume that the circulation distribution of the aerofoil 1 or 3 and that of the aerofoil 2 when placed individually are

$$\Gamma_1 = \Gamma_{01}\sqrt{1-\eta^2} \quad \text{and} \quad \Gamma_2 = \Gamma_{02}\sqrt{1-\xi^2}, \quad \cdots\cdots \quad (16)$$

where $\eta = \frac{y}{s_1}$, $\zeta = \frac{y}{s_2}$, s_1 the semi-span of the aerofoil 1, s_2 the semi-span of the aerofoil 2, and the origins of the η- and ξ-axes lie at the centres of the aerofoils 1 and 2 respectively.

The induced velocity due to this distribution of circulation is obviously as follows:

$$\left.\begin{aligned} &\text{for } |y| \leqq s_1, \qquad w = \frac{\Gamma_{01}}{4s_1}, \\ &\text{for } |y| > s_1, \qquad w = -\frac{\Gamma_{01}}{4s_1}\left\{\frac{y}{\sqrt{y^2-s_1^2}} - 1\right\} \end{aligned}\right\} \quad \cdots\cdots \quad (17)$$

If the origin is taken at the centre of the aerofoil 1 as shown in Fig. 9, the induced velocities on the aerofoil 1 due to the aerofoil 2 and due to the aerofoil 3 are immediately obtained from the equation (17), i.e.,

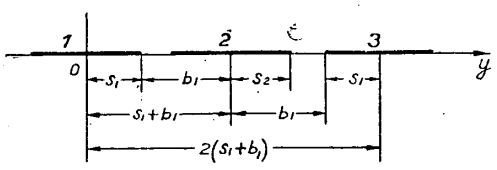

Fig. 9.

$$w_{12} = -\frac{\Gamma_{02}}{4s_2}\left\{\frac{\xi_0-\xi}{\sqrt{(\xi_0-\xi)^2-1}}-1\right\} \quad \cdots\cdots\cdots \quad (18)$$

and

$$w_{13} = -\frac{\Gamma_{01}}{4s_1}\left\{\frac{\eta_0-\eta}{\sqrt{(\eta_0-\eta)^2-1}}-1\right\}, \quad \cdots\cdots\cdots \quad (19)$$

where $\xi_0 = \frac{s_1+b_1}{s_2}$, $\xi = \eta\frac{s_1}{s_2}$ and $\eta_0 = \frac{2(s_1+b_1)}{s_1}$.

It follows that the total induced velocity on the aerofoil 1 becomes

$$\begin{aligned} w_1 &= w_{11}+w_{12}+w_{13} \\ &= \frac{\Gamma_{01}}{2s_1}+\frac{\Gamma_{02}}{4s_2}-\frac{\Gamma_{02}}{4s_2}\cdot\frac{\xi_0-\xi}{\sqrt{(\xi_0-\xi)^2-1}}-\frac{\Gamma_{01}}{4s_1}\cdot\frac{\eta_0-\eta}{\sqrt{(\eta_0-\eta)^2-1}} \quad \cdots \quad (20) \end{aligned}$$

Then, the circulation of the aerofoil 1 becomes

$$\begin{aligned} \Gamma_1^* &= \Gamma_1+\frac{\partial\Gamma_1}{\partial\alpha}\cdot\frac{|w_{12}|+|w_{13}|}{V} \\ &= \Gamma_{01}\sqrt{1-\eta^2}+\frac{\partial\Gamma_{01}}{\partial\alpha}\sqrt{1-\eta^2}\cdot\frac{1}{V} \\ &\quad\times\left[\frac{\Gamma_{02}}{4s_2}\left\{\frac{\xi_0-\xi}{\sqrt{(\xi_0-\xi)^2-1}}-1\right\}+\frac{\Gamma_{01}}{4s_1}\left\{\frac{\eta_0-\eta}{\sqrt{(\eta_0-\eta)^2-1}}-1\right\}\right] \end{aligned}$$

Considering that

$$\frac{\partial\Gamma_{01}}{\partial\alpha} = \frac{1}{1+\frac{c_1}{2\lambda_1}}Vt_1c_1, \quad \cdots\cdots\cdots\cdots \quad (21)$$

where $c_1 = \frac{1}{2}\frac{\partial C_{z\infty 1}}{\partial\alpha}$, $\lambda_1 = \frac{2s_1}{t_1}$ and t_1 is the chord length of the aerofoil 1, then the above equation becomes

$$\begin{aligned} \Gamma_1^* &= \Gamma_{01}\sqrt{1-\eta^2}+\frac{\frac{c_1}{2\lambda_1}}{1+\frac{c_1}{2\lambda_1}}\Gamma_{01}\sqrt{1-\eta^2}\left\{\frac{\eta_0-\eta}{\sqrt{(\eta_0-\eta)^2-1}}-1\right\} \\ &\quad+\frac{\frac{c_1}{2\lambda_1'}}{1+\frac{c_1}{2\lambda_1}}\Gamma_{02}\sqrt{1-\eta^2}\left\{\frac{\xi_0-\xi}{\sqrt{(\xi_0-\xi)^2-1}}-1\right\}, \quad \cdots\cdots \quad (22) \end{aligned}$$

where $\lambda'_1 = \dfrac{2s_2}{t_1}$.

If the origin is taken at the centre of the aerofoil 2 as shown in Fig. 10, the induced velocities on the aerofoil 2 due to the aerofoil 1 and due to the aerofoil 3 are immediately obtained from the equation (21), i.e.,

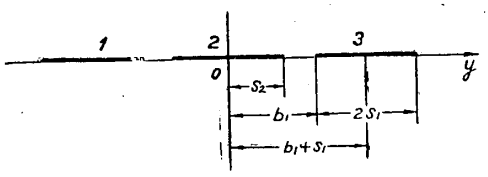

Fig. 10.

$$w_{21} = -\frac{\Gamma_{01}}{4s_1}\left\{\frac{\eta_1+\eta}{\sqrt{(\eta+\eta)^2-1}}-1\right\}, \quad \cdots\cdots\cdots \quad (23)$$

$$w_{23} = -\frac{\Gamma_{01}}{4s_1}\left\{\frac{\eta_1-\eta}{\sqrt{\eta_1-\eta)^2-1}}-1\right\}, \quad \cdots\cdots\cdots \quad (24)$$

where $\eta = \dfrac{y}{s_1}$ and $\eta_1 = \dfrac{b_1+s_1}{s_1}$. Hence, the total induced velocity on the aerofoil 2 becomes

$$w_2 = w_{22}+w_{21}+w_{23}$$

$$= \frac{\Gamma_{02}}{4s_2}+\frac{\Gamma_{01}}{2s_1}-\frac{\Gamma_{01}}{4s_1}\left\{\frac{\eta_1+\eta}{\sqrt{(\eta_1+\eta)^2-1}}+\frac{\eta_1-\eta}{\sqrt{(\eta_1-\eta)^2-1}}\right\} \quad \cdots\cdots \quad (25)$$

The circulation of the aerofoil 2 becomes

$$\Gamma_2^* = \Gamma_2+\frac{\partial\Gamma_2}{\partial\alpha}\cdot\frac{|w_{21}|+|w_{23}|}{V}$$

$$= \Gamma_{02}\sqrt{1-\xi^2}+\frac{\partial\Gamma_{02}}{\partial\alpha}\sqrt{1-\xi^2}\cdot\frac{\Gamma_{01}}{4s_1V}\left\{\frac{\eta_1+\eta}{\sqrt{(\eta_1+\eta)^2-1}}+\frac{\eta_1-\eta}{\sqrt{(\eta_1-\eta)^2-1}}-2\right\}.$$

Considering that

$$\frac{\partial\Gamma_{02}}{\partial\alpha} = \frac{1}{1+\dfrac{c_2}{2\lambda_2}}c_2 Vt_2,$$

where $c_2 = \dfrac{1}{2}\dfrac{\partial C_{z\infty 2}}{\partial\alpha}$ and $\lambda_2 = \dfrac{2s_2}{t_2}$, then the above equation becomes

$$\Gamma_2^* = \Gamma_{02}\sqrt{1-\xi^2} + \frac{\frac{c_2}{2\lambda_2'}}{1+\frac{c_2}{2\lambda_2}}\Gamma_{01}\sqrt{1-\xi^2} \times \left\{\frac{\eta_1+\eta}{\sqrt{(\eta_1+\eta)^2-1}} + \frac{\eta_1-\eta}{\sqrt{(\eta_1-\eta)^2-1}} - 2\right\}, \quad \cdots\cdots \quad (26)$$

where $\lambda_2' = \frac{2s_1}{t_2}$. The circulation of the aerofoil 3 can be immediately obtained by putting $-y$ in place of y in the eq. (22).

If we denote the lift of the aerofoil 1 by L_1^*, then we get

$$L_1^* = \int_{-s_1}^{+s_1} \rho V \Gamma_1^* dy = \rho V s_1 \int_{-1}^{+1} \Gamma_1^* d\eta$$

$$= \frac{1}{2}\pi\rho V s_1 \Gamma_{01}\left[1 + \frac{\frac{c_1}{2\lambda_1}}{1+\frac{c_1}{2\lambda_1}}\left\{\frac{2}{\pi}I_1 - 1\right\} + \frac{\frac{c_1}{2\lambda_1'}}{1+\frac{c_1}{2\lambda_1}}\cdot\frac{\Gamma_{02}}{\Gamma_{01}}\left\{\frac{2}{\pi}I_2 - 1\right\}\right], \quad \cdots\cdots \quad (27)$$

where

$$I_1 = \int_{-1}^{+1}\sqrt{1-\eta^2}\cdot\frac{\eta_0-\eta}{\sqrt{(\eta_0-\eta)^2-1}}d\eta, \quad \cdots\cdots \quad (28)$$

$$I_2 = \int_{-1}^{+1}\sqrt{1-\eta^2}\cdot\frac{\xi_0-\xi}{\sqrt{(\xi_0-\xi)^2-1}}d\eta. \quad \cdots\cdots \quad (29)$$

The lifts of the aerofoils 1 and 2 when placed individually are, respectively,

$$L_1 = \frac{1}{2}\pi\rho V s_1 \Gamma_{01}, \qquad L_2 = \frac{1}{2}\pi\rho V s_2 \Gamma_{02}. \quad \cdots\cdots \quad (30)$$

Hence

$$\frac{\Gamma_{02}}{\Gamma_{01}} = \frac{L_2}{L_1}\cdot\frac{s_1}{s_2} \quad \cdots\cdots \quad (31)$$

Therefore, the equation (31) becomes

$$L_1^* = L_1\left[1 + \frac{\frac{c_1}{2\lambda_1}}{1+\frac{c_1}{2\lambda_1}}\left\{\frac{2}{\pi}I_1 - 1\right\} + \frac{\frac{c_1}{2\lambda_1'}}{1+\frac{c_1}{2\lambda_1}}\cdot\frac{L_2 s_1}{L_1 s_2}\left\{\frac{2}{\pi}I_2 - 1\right\}\right] \quad (32)$$

Now, we shall evaluate the integral I_1. Since $|\eta_0|>2$ and $|\eta|\leqq 1$, we get the following expansion

$$\frac{\eta_0-\eta}{\sqrt{(\eta_0-\eta)^2-1}} = 1+\sum_{n=1}^{\infty}\frac{1\cdot3\cdot5\ldots(2n-1)}{2^n n!}\cdot\frac{1}{(\eta_0-\eta)^{2n}}$$

Hence $$I_1 = \int_{-1}^{+1}\sqrt{1-\eta^2}\,d\eta+\sum_{n=1}^{\infty}\frac{1\cdot3\cdot5\ldots(2n-1)}{2^n n!}\int_{-1}^{+1}\frac{\sqrt{1-\eta^2}}{(\eta_0-\eta)^{2n}}d\eta\,.$$

Put $\eta=\cos\theta$. Then

$$\int_{-1}^{+1}\frac{\sqrt{1-\eta^2}}{(\eta_0-\eta)^{2n}}d\eta = \int_0^{\pi}\frac{\sin^2\theta}{(\eta_0-\cos\theta)^{2n}}d\theta$$

Write $$G_m = \int_0^{\pi}\frac{\sin^2\theta}{(\eta_0-\cos\theta)^m}d\theta \quad\ldots\ldots\ldots\ldots\ldots \quad (33)$$

The cases of $m=0$ and 1 can be easily evaluated.

$$G_0 = \int_0^{\pi}\sin^2\theta\,d\theta = \frac{\pi}{2} \quad\ldots\ldots\ldots\ldots\ldots\ldots \quad (34)$$

$$G_1 = \int_0^{\pi}\frac{\sin^2\theta}{\eta_0-\cos\theta}d\theta = \pi(\eta_0-\sqrt{\eta_0-1})\ldots\ldots\ldots \quad (35)$$

The values of G_2, G_3 ... can be obtained by the following recurrence formula (Reference 2)

$$G_m = \frac{2m-5}{m-1}\cdot\frac{\eta_0}{\eta_0^2-1}G_{m-1}+\frac{4-m}{m-1}\cdot\frac{1}{\eta_0^2-1}G_{m-2}\ldots\ldots \quad (36)$$

Hence, the integral I_1 can be written in the form

$$I_1 = \frac{\pi}{2}+\sum_{n=1}^{\infty}\frac{1\cdot3\cdot5\ldots(2n-1)}{2^n n!}G_{2n}\ldots\ldots\ldots \quad (37)$$

Secondly, we shall evaluate the integral I_2. Since $\xi=\frac{y}{s_2}=\frac{s_1}{s_2}\eta$ and $\xi_0=\frac{s_1+b_1}{s_2}$, we have the following expansion

$$\frac{\xi_0-\xi}{\sqrt{(\xi^0-\xi)^2-1}} = 1+\sum_{n=1}^{\infty}\frac{1\cdot3\cdot5\ldots(2n-1)}{2^n n!}\cdot\frac{1}{\nu^{2n}(\eta_1-\eta)^{2n}},$$

where $\nu=\frac{s_1}{s_2}$ and $\eta_1=\frac{s_1+b_1}{s_1}$. Hence

$$I_2=\int_{-1}^{+1}\sqrt{1-\eta^2}\left[1+\sum_{n=1}^{\infty}\frac{1\cdot3\cdot5\ldots(2n-1)}{2^n n!}\cdot\frac{1}{\nu^{2n}(\eta_1-\eta)^{2n}}\right]d\eta$$

$$=\frac{\pi}{2}+\sum_{n=1}^{\infty}\frac{1\cdot3\cdot5\ldots(2n-1)}{2^n n!\,\nu^{2n}}\int_{-1}^{+1}\frac{\sqrt{1-\eta^2}}{(\eta_1-\eta)^{2n}}d\eta \quad \ldots\ldots\ldots \quad (38)$$

The integration which occurs in the equation (38) is the same as G_{2n} when we put η_1 in place of η_0.

The lift of the aerofoil 2 is

$$L_2^*=\int_{-s_2}^{s_2}\rho V\Gamma_2^*dy=\rho Vs_2\int_{-1}^{+1}\Gamma_1^*d\xi$$

$$=\rho Vs_2\int_{-1}^{+1}\left[\Gamma_{02}\sqrt{1-\xi^2}+\frac{\frac{c_2}{2\lambda_2'}}{1+\frac{c_2}{2\lambda_2}}\Gamma_{01}\sqrt{1-\xi^2}\right.$$

$$\left.\times\left\{\frac{\eta_1+\eta}{\sqrt{(\eta_1+\eta)^2-1}}+\frac{\eta_1-\eta}{\sqrt{(\eta_1-\eta)^2-1}}-2\right\}\right]d\xi.$$

The integrals $\int_{-1}^{+1}\sqrt{1-\xi^2}\cdot\frac{\eta_1+\eta}{\sqrt{(\eta_1+\eta)^2-1}}d\xi$ and $\int_{-1}^{+1}\sqrt{1-\xi^2}\cdot\frac{\eta_1-\eta}{\sqrt{(\eta_1-\eta)^2-1}}d\xi$ are the same, for the latter can be derived from the former by putting $-y$ in place of y.

Write
$$I_3=\int_{-1}^{+1}\sqrt{1-\xi^2}\cdot\frac{\eta_1+\eta}{\sqrt{(\eta_1+\eta)^2-1}}d\xi$$

$$=\int_{-1}^{+1}\sqrt{1-\xi^2}\frac{\eta_1-\eta}{\sqrt{(\eta_1-\eta)^2-1}}d\xi \quad \ldots\ldots\ldots \quad (39)$$

Then, the lift of the aerofoil 2 becomes

$$L_2^* = \frac{1}{2}\pi\rho V s_2 \Gamma_{02}\left[1+\frac{\frac{c_2}{\lambda_2'}}{1+\frac{c_2}{2\lambda_2}}\cdot\frac{\Gamma_{01}'}{\Gamma_{02}}\left(\frac{2}{\pi}I_3-1\right)\right] \quad \cdots\cdots \quad (40)$$

Introducing the equations (30) and (31), then we get

$$L_2^* = L_2\left[1+\frac{\frac{c_2}{\lambda_2'}}{1+\frac{c_2}{2\lambda_2}}\cdot\frac{L_1 s_2}{L_2 s_1}\left(\frac{2}{\pi}I_3-1\right)\right] \quad \cdots\cdots\cdots \quad (41)$$

Since $\xi = \frac{y}{s_2}$, $\eta_1 = \frac{b_1+s_1}{s_1}$, $\eta = \frac{y}{s_1} = \frac{\xi}{\nu}$ and $\nu\eta_1 = \frac{b_1+s_1}{s_2} = \xi_0$, so we have the following expansion

$$\frac{\eta_1-\eta}{\sqrt{(\eta_1-\eta)^2-1}} = 1+\sum_{n=1}^{\infty}\frac{1\cdot3\cdot5\cdots(2n-1)}{2^n n!}\cdot\frac{\nu^{2n}}{(\xi_0-\xi)^{2n}}.$$

Hence $$I_3 = \frac{\pi}{2}+\sum_{n=1}^{\infty}\frac{1\cdot3\cdot5\cdots(2n-1)}{2^n n!}\nu^{2n}\int_{-1}^{+1}\frac{\sqrt{1-\xi^2}}{(\xi_0-\xi)^{2n}}d\xi \quad \cdots\cdots \quad (42)$$

The integral $\int_{-1}^{+1}\frac{\sqrt{1-\xi^2}}{(\xi_0-\xi)^{2n}}d\xi$ which occurs in the above equation is of of the same form as G_{2n} which has been seen in the evaluation of I_1.

The induced drag of the aerofoil 1, D_{i1}^* say, is obtained by the equation

$$D_{i1}^* = \int_{-s_1}^{s_1}\rho w_1 \Gamma_1^* dy, \quad \cdots\cdots\cdots\cdots \quad (43)$$

Substituting $$w_1 = w_{11}+w_{12}+w_{13}$$

$$\Gamma_1^* = \Gamma_1+\Delta\Gamma_{12}+\Delta\Gamma_{13}$$

in the above equation and ignoring the small quantities $\Delta\Gamma_{12}w_{12}$, $\Delta\Gamma_{12}w_{13}$, $\Delta\Gamma_{13}w_{12}$ and $\Delta\Gamma_{13}w_{13}$, then we get

$$D_{i1}^{*}=\int_{-1}^{+1}\rho s_1\left\{w_{11}\Gamma_1^{*}+\Gamma_1(w_{12}+w_{13})\right\}d\eta$$

$$=\frac{1}{8}\pi\rho\Gamma_{01}^{2}\left[1-\left(\frac{2}{\pi}I_1-1\right)\left(1-\frac{\frac{c_1}{2\lambda_1}}{1+\frac{c_1}{2\lambda_1}}\right)\right.$$

$$\left.-\frac{s_1\Gamma_{02}}{s_2\Gamma_{01}}\left(\frac{2}{\pi}I_2-1\right)\left(1-\frac{s_2}{s_1}\cdot\frac{\frac{c_1}{2\lambda_1'}}{1+\frac{c_1}{2\lambda_1}}\right)\right] \quad \cdots\cdots \quad (44)$$

Introducing the equations (30) and (31), then the equation (44) can be rewritten in the form

$$D_{i1}^{*}=\frac{L_1^2}{2\pi\rho V^2 s_1^2}\left[1-\left(\frac{2}{\pi}I_1-1\right)\left(1-\frac{\frac{c_1}{2\lambda_1}}{1+\frac{c_1}{2\lambda_1}}\right)\right.$$

$$\left.-\frac{s_1^2L_2}{s_2^2L_1}\left(\frac{2}{\pi}I_2-1\right)\left(1-\frac{s_2}{s_1}\cdot\frac{\frac{c_1}{2\lambda_1'}}{1+\frac{c_1}{2\lambda_1}}\right)\right] \quad \cdots\cdots \quad (45)$$

The induced drag of the aerofoil 2, D_{i1}^{*} say, is calculated by the equation

$$D_{i2}^{*}=\int_{-s_2}^{s_2}\rho w_2\Gamma_2^{*}dy \quad \cdots\cdots\cdots\cdots \quad (46)$$

Substituting $\quad w_2=w_{21}+w_{22}+w_{23}$

$$\Gamma_2^{*}=\Gamma_2+\Delta\Gamma_{21}+\Delta\Gamma_{23}$$

in the above equation and ignoring the small quantities $\Delta\Gamma_{21}w_{21}$, $\Delta\Gamma_{21}w_{23}$, $\Delta\Gamma_{23}w_{21}$ and $\Delta\Gamma_{23}w_{23}$, then we get

$$D_{i2}^{*}=\rho s_2\int_{-1}^{+1}\left\{w_{22}\Gamma_2^{*}+\Gamma_2(w_{21}+w_{23})\right\}d\xi$$

$$=\frac{1}{8}\pi\rho\Gamma_{02}^{2}\left[1-\frac{2s_2\Gamma_{01}}{s_1L_{02}}\left(\frac{2}{\pi}I_3-1\right)\left(1-\frac{s_1}{s^2}\cdot\frac{\frac{c_2}{2\lambda_2'}}{1+\frac{c_2}{2\lambda_2}}\right)\right]\cdots\cdots\quad(47)$$

Introducing the equations (30) and (31), then the above equation can be rewritten in the form

$$D_{i2}^{*}=\frac{L_2^2}{2\pi\rho V^2s_2^2}\left[1-\frac{2s_2^2L_1}{s_1^2L_2}\left(\frac{2}{\pi}I_3-1\right)\left(1-\frac{s_1}{s_2}\cdot\frac{\frac{c_2}{2\lambda_2'}}{1+\frac{c_2}{2\lambda_2}}\right)\right]\cdots\quad(48)$$

§2.2. *Aerofoil with one longitudinal slot.*

If we put $s_2=0$ $t_2=0$ and $\Gamma_{02}=0$ in the expressions obtained in the preceding article, we have the solution of the divided aerofoil as shown in Fig. 11.

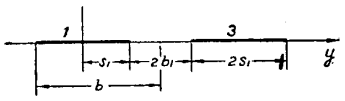

Fig. 11.

The induced velocity, the circulation and the lift of the aerofoil 1 are, from equations (21), (22) and (27),

$$w_1=w_{11}+w_{12}=\frac{\Gamma_{01}}{4s_1}\left\{2-\frac{\eta_0-\eta}{\sqrt{(\eta_0-\eta)^2-1}}\right\},\quad\cdots\cdots\quad(49)$$

$$\Gamma_1^{*}=\Gamma_{01}\sqrt{1-\eta^2}\left[1+\frac{\frac{c_1}{2\lambda_1}}{1+\frac{c_1}{2\lambda_1}}\left\{\frac{\eta_0-\eta}{\sqrt{(\eta_0-\eta)^2-1}}-1\right\}\right]\cdots\quad(50)$$

$$L^{*}=\frac{1}{2}\pi\rho Vs_1\Gamma_{01}\left[1+\frac{\frac{c_1}{2\lambda_1}}{1+\frac{c_1}{2\lambda_1}}\left(\frac{2}{\pi}I_1-1\right)\right]\cdots\cdots\quad(51)$$

The values of the integral I_1 are shown in Table 3 and Fig. 12 as the function of $k(= b_1/b = b_1/(4s_1+b_1))$.

TABLE 3.

k	0	0·05	0·1	0·2	0·3	0·4	0·5	0·6	0·7	0·8
I_1	1·9728	1·8280	1·7557	1·6774	1·6351	1·6097	1·5936	1·5834	1·5766	1·5732

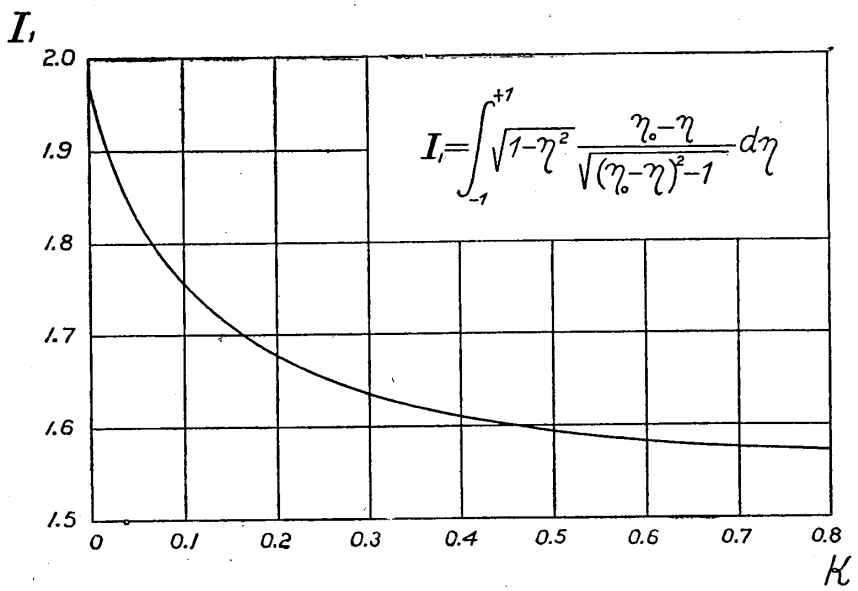

Fig. 12.

The lift of the aerofoil 1 when placed individually becomes

$$L = \frac{1}{2}\pi\rho V s_1 \Gamma_{01} .$$

Therefore, the ratio of the lift of the aerofoil 1 to that of the aerofoil when placed individually is

$$\mathfrak{L} = \frac{L^*}{L} = 1 + \frac{\frac{c_1}{2\lambda_1}}{1+\frac{c_1}{2\lambda_1}}\left(\frac{2}{\pi}I_1 - 1\right). \quad \cdots\cdots \quad (52)$$

Then, the lift coefficient of the divided aerofoil, C_z' say, becomes

$$C_z' = \mathfrak{L} C_z , \quad \cdots\cdots\cdots\cdots\cdots\cdots \quad (53)$$

where C_z is the lift coefficient of the aerofoil when placed individually.

The induced drag of the aerofoil 1 becomes from the equation (45)

$$D_i^* = \frac{L^2}{\pi\rho V^2 s_1^2}\left[1 - \frac{I_1}{\pi} + \frac{\frac{c_1}{2\lambda_1}}{1+\frac{c_1}{2\lambda_1}}\left(\frac{I_1}{\pi} - \frac{1}{2}\right)\right], \quad \cdots\cdots \quad (54)$$

and that of the aerofoil 1 when placed individually is

$$D_i = \frac{L^2}{2\pi\rho V^2 s_1^2} .$$

The ratio of the induced drag of the aerofoil 1 to that of the aerofoil when placed individually is

$$\mathfrak{D} = \frac{D_i^*}{D_i} = 2\left[1 - \frac{I_1}{\pi} + \frac{\frac{c_1}{2\lambda_1}}{1+\frac{c_1}{2\lambda_1}}\left(\frac{I_1}{\pi} - \frac{1}{2}\right)\right] \cdots\cdots\cdots \quad (55)$$

If C_{xp} is the profile drag coefficient of the aerofoil 1 when placed individually, then the total drag coefficient of the divided aerofoil becomes

$$C_x' = C_{x_p} + \mathfrak{D} C_{x_i} . \quad \cdots\cdots\cdots\cdots\cdots \quad (56)$$

In order to confirm the calculation, the wind-tunnel experiment is carried out with regard to the divided aerofoil of $k = 0{\cdot}2$, whose original aerofoil is 75 cm × 15 cm rectangular aerofoil of Göttingen 593 section, under about 30 m/s wind velocity. The results of calculation agree satisfactorily with the experimental results, as shown in Fig. 13*b*.

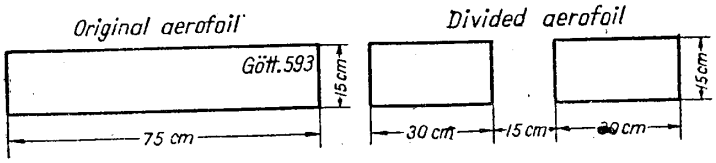

Fig. 13 a. Divided aerofoil tested.

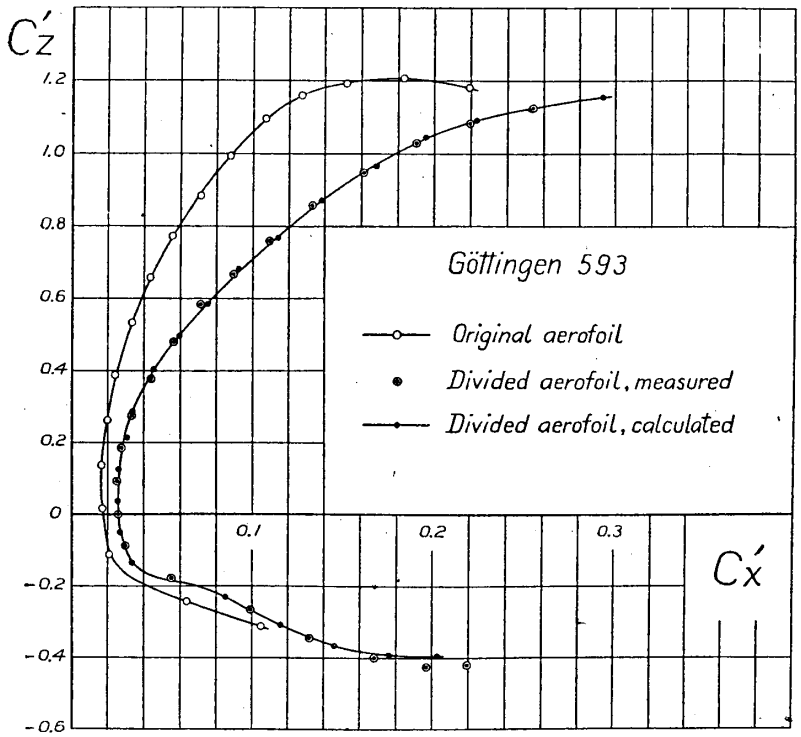

Fig. 13 b. Comparison of the calculated result with the experimental result.

§2.3. *Case when the two longitudinal slots vanish.* (*Aerofoil with two discontinuities*).

When the two longitudinal slots in the aerofoil which has been studied in §2·1 vanish, we have the aerofoil with two discontinuities across the span as shown in Fig. 14. Hence, putting $s_2 = b_1$ in the equations obtained in §2·1, then we get the solution for the aerofoil with two discontinuities.

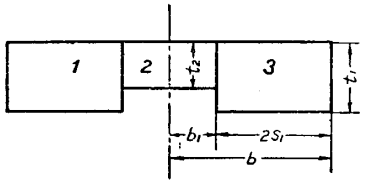

Ftg. 14.

The induced velocities of the aerofoil portions 1 and 2 are from the equations (20) and (25)

$$\left.\begin{aligned} w_1 &= \frac{\Gamma_{01}}{2s_1} + \frac{\Gamma_{02}}{4b_1} - \frac{\Gamma_{02}}{4b_1}\cdot\frac{\xi_0-\xi}{\sqrt{(\xi_0-\xi)^2-1}} - \frac{\Gamma_{01}}{4s_1}\cdot\frac{\eta_0-\eta}{\sqrt{(\eta_0-\eta)^2-1}}, \\ w_2 &= \frac{\Gamma_{02}}{4b_1} + \frac{\Gamma_{01}}{2s_1} - \frac{\Gamma_{01}}{4s_1}\left\{\frac{\eta_1+\eta}{\sqrt{(\eta_1+\eta)^2-1}} + \frac{\eta_1-\eta}{\sqrt{(\eta_1-\eta)^2-1}}\right\}, \end{aligned}\right\} \quad (57)$$

where $\xi_0 = \dfrac{s_1 + b_1}{b_1}$, $\eta_0 = \dfrac{2(s_1+b_1)}{s_1}$ and $\eta_1 = \dfrac{b_1 + s_1}{s_2}$.

The circulations of the aerofoil portions 1 and 2 are from the equations (22) and (26)

$$\left.\begin{aligned}
\Gamma_1^* &= \Gamma_{01}\sqrt{1-\eta^2} + \frac{\dfrac{c_1}{2\lambda_1}}{1+\dfrac{c_1}{2\lambda_1}}\Gamma_{01}\sqrt{1-\eta^2}\left\{\frac{\eta_0-\eta}{\sqrt{(\eta_0-\eta)^2-1}}-1\right\} \\
&\quad + \frac{\dfrac{c_1}{2\lambda_1'}}{1+\dfrac{c_1}{2\lambda_1}}\Gamma_{02}\sqrt{1-\eta^2}\left\{\frac{\xi_0-\xi}{\sqrt{(\xi_0-\xi)^2-1}}-1\right\}, \\
\Gamma_2^* &= \Gamma_{02}\sqrt{1-\xi^2} + \frac{\dfrac{c_2}{2\lambda_2'}}{1+\dfrac{c_2}{2\lambda_2}}\Gamma_{01}\sqrt{1-\xi^2} \\
&\quad \times\left\{\frac{\eta_1+\eta}{\sqrt{(\eta_1+\eta)^2-1}}+\frac{\eta_1-\eta}{\sqrt{(\eta_1-\eta)^2-1}}-2\right\},
\end{aligned}\right\} \quad (58)$$

where $\lambda_1 = \dfrac{2s_1}{t_1}$, $\lambda_1' = \dfrac{2b_1}{t_1}$, $\lambda_2 = \dfrac{2b_1}{t_2}$ and $\lambda_2' = \dfrac{2s_1}{t_2}$.

The total lift and the total induced drag of the aerofoil with discontinuities, L and D_i, are obtained by $2L_1^* + L_2^*$ and $2D_{i1}^* + D_{i2}^*$ respectively, i.e.,

$$\begin{aligned}
L = 2L_1\left\{1+\frac{\dfrac{c_1}{2\lambda_1}}{1+\dfrac{c_1}{2\lambda_1}}\left(\frac{2}{\pi}I_1-1\right)+\frac{\dfrac{c_1}{2\lambda_1'}}{1+\dfrac{c_1}{2\lambda_1}}\cdot\frac{L_2s_1}{L_1b_1}\left(\frac{2}{\pi}I_2-1\right)\right\} \\
+L_2\left\{1+\frac{\dfrac{c_2}{2\lambda_2'}}{1+\dfrac{c_2}{2\lambda_2}}\cdot\frac{L_1b_1}{L_2s_1}\left(\frac{2}{\pi}I_3-1\right)\right\} \quad \cdots\cdots \quad (59)
\end{aligned}$$

$$D_i = 2D_{i1}\left\{1-\left(\frac{2}{\pi}I_1-1\right)\left(1-\frac{\frac{c_1}{2\lambda_1}}{1+\frac{c_1}{2\lambda_1}}\right)\right.$$
$$\left.-\frac{s_1^2L_2}{b_1^2L_1}\left(\frac{2}{\pi}I_2-1\right)\left(1-\frac{b_1}{s_1}\cdot\frac{\frac{c_1}{2\lambda_1'}}{1+\frac{c_1}{2\lambda_1}}\right)\right\}$$
$$+D_{i2}\left\{1-\frac{2b_1^2L_1}{s_1^2L_2}\left(\frac{2}{\pi}I_3-1\right)\left(1-\frac{s_1}{b^1}\cdot\frac{\frac{c_2}{2\lambda_2'}}{1+\frac{c_2}{2\lambda_2}}\right)\right\}\cdots \quad (60)$$

Let $$L_1=C_{z_1}\frac{\rho V^2}{2}S_1, \qquad D_{i1}=C_{x_{i1}}\frac{\rho V^2}{2}S_1,$$
$$L_2=C_{z_2}\frac{\rho V^2}{2}S_2, \qquad D_{i2}=C_{x_{i2}}\frac{\rho V^2}{2}S_2.$$

Then, the lift coefficient and the induced drag coefficient of the aerofoil with two discontinuities, referred to the wing area of the original aerofoil S, are

$$C_z = 2C_{z_1}\frac{S_1}{S}\left\{1+\frac{\frac{c_1}{2\lambda_1}}{1+\frac{c_1}{2\lambda_1}}\left(\frac{2}{\pi}I_1-1\right)+\frac{\frac{c_1}{2\lambda_1'}}{1+\frac{c_1}{2\lambda_1}}\cdot\frac{L_2}{L_1}\left(\frac{2}{\pi}I_2-1\right)\right\}$$
$$+C_{z_2}\frac{S_2}{S}\left\{1+\frac{\frac{c_2}{\lambda_2'}}{1+\frac{c_2}{2\lambda_2}}\cdot\frac{L_1b_1}{L_2s_1}\left(\frac{2}{\pi}I_3-1\right)\right\}$$

$$C_{x_i} = 2C_{x_{i1}}\frac{S_1}{S}\left\{1-\left(\frac{2}{\pi}I_1-1\right)\left(1-\frac{\frac{c_1}{2\lambda_1}}{1+\frac{c_1}{2\lambda_1}}\right)\right.$$
$$\left.-\frac{s_1^2L_2}{b_1^2L_1}\left(\frac{2}{\pi}I_2-1\right)\left(1-\frac{b_1}{s_1}\cdot\frac{\frac{c_1}{2\lambda_1'}}{1+\frac{c_1}{2\lambda_1}}\right)\right\}$$

$$+C_{x_{i2}}\frac{S_2}{S}\left\{1-\frac{2b_1^2L_1}{s_1^2L_2}\left(\frac{2}{\pi}I_3-1\right)\left(1-\frac{s_1}{b_1}\cdot\frac{\frac{c_2}{2\lambda_2'}}{1+\frac{c_2}{2\lambda_2}}\right)\right\}.$$

Substituting the following equations

$$\frac{L_2s_1}{L_1b_1}=(1-\tau)\frac{1+\frac{c_1}{2\lambda_1}}{1+\frac{c_2}{2\lambda_2}}\cdot\frac{C_{z_{2\infty}}}{C_{z_{1\infty}}},\qquad \frac{L_2s_1^2}{L_1b_1^2}=\frac{\lambda_1}{\lambda_2}\cdot\frac{1+\frac{c_1}{2\lambda_1}}{1+\frac{c_2}{2\lambda_2}}\cdot\frac{C_{z_{2\infty}}}{C_{z_{1\infty}}},$$

$$\frac{S_1}{S}=\frac{1-k}{2},\qquad \frac{S_2}{S}=k(1-\tau),\qquad \frac{s_1}{b_1}=\frac{1-k}{2k},$$

where $k=\frac{b_1}{b}$ and $\tau=\frac{t_1-t_2}{t_1}$, into the above equations, then we get

$$C_z=C_{z_1}(1-k)\left\{1+\frac{\frac{c_1}{2\lambda_1}}{1+\frac{c_1}{2\lambda_1}}\left(\frac{2}{\pi}I_1-1\right)+\frac{\frac{c_1}{2\lambda_1'}}{1+\frac{c_2}{2\lambda_2}}(1-\tau)\frac{C_{z_{2\infty}}}{C_{z_{1\infty}}}\left(\frac{2}{\pi}I_2-1\right)\right\}$$

$$+C_{z_2}k(1-\tau)\left\{1+\frac{1}{1-\tau}\cdot\frac{\frac{c_2}{\lambda_2'}}{1+\frac{c_1}{2\lambda_1}}\cdot\frac{c_{z_{1\infty}}}{c_{z_{2\infty}}}\left(\frac{2}{\pi}I_3-1\right)\right\}\ldots. \quad (61)$$

$$C_{x_i}=C_{x_{i_1}}(1-k)\left\{1-\left(\frac{2}{\pi}I_1-1\right)\left(1-\frac{\frac{c_1}{2\lambda_1}}{1+\frac{c_1}{2\lambda_1}}\right)\right.$$

$$\left.-\frac{\lambda_1}{\lambda_2}\cdot\frac{1+\frac{c_1}{2\lambda_1}}{1+\frac{c_2}{2\lambda_2}}\cdot\frac{C_{z_{2\infty}}}{C_{z_1\infty}}\left(\frac{2}{\pi}I_2-1\right)\left(1-\frac{2k}{1-k}\cdot\frac{\frac{c_1}{2\lambda_1'}}{1+\frac{c_1}{2\lambda_1}}\right)\right\}$$

$$+C_{x_{i2}}k(1-\tau)\left\{1-\frac{2\lambda_2}{\lambda_1}\cdot\frac{1+\frac{c_2}{2\lambda_2}}{1+\frac{c_1}{2\lambda_1}}\cdot\frac{C_{z_{1\infty}}}{C_{z_{2\infty}}}\left(\frac{2}{\pi}I_3-1\right)\right.$$

$$\left.\times\left(1-\frac{1-k}{2k}\cdot\frac{\frac{c_2}{2\lambda_2'}}{1+\frac{c_2}{2\lambda_2}}\right)\right\} \quad \cdots\cdots\cdots\cdots \quad (62)$$

The lift coefficient and the induced drag coefficient of the aerofoil without discontinuities or the original aerofoil, $\bar{C}_z$ and $\bar{C}_{xi}$, are obtained by putting $L_2=0$, $t_2=b_1=0$ and $2s_1=b$ in the above equations.

$$\left.\begin{aligned}\bar{C}_z&=\bar{C}_{z_1}\left\{1+\frac{\frac{c_1}{2\bar{\lambda}_1}}{1+\frac{c_1}{2\bar{\lambda}_1}}\left(\frac{2}{\pi}\bar{I}_1-1\right)\right\},\\ \bar{C}_{x_i}&=2\bar{C}_{x_{i1}}\left\{1-\frac{\bar{I}_1}{\pi}+\frac{\frac{c_1}{2\bar{\lambda}_1}}{1+\frac{c_1}{2\bar{\lambda}_1}}\left(\frac{\bar{I}_1}{\pi}-\frac{1}{2}\right)\right\},\end{aligned}\right\} \quad \cdots\cdots \quad (63)$$

where the bar sign denotes the values for the case of $2s_1=b$.

Considering the following relations

$$\frac{C_{z_1}}{\bar{C}_{z_1}}=\frac{1+\frac{c_1}{2\bar{\lambda}_1}}{1+\frac{c_1}{2\lambda_1}}, \qquad \frac{C_{z_2}}{\bar{C}_{z_1}}=\frac{1+\frac{c_1}{2\bar{\lambda}_1}}{1+\frac{c_2}{2\lambda_2}}\cdot\frac{C_{z_{2\infty}}}{C_{z_{1\infty}}},$$

$$\frac{C_{x_{i1}}}{\bar{C}_{x_{i1}}}=\left\{\frac{1+\frac{c_1}{2\bar{\lambda}_1}}{1+\frac{c_1}{2\lambda_1}}\right\}^2\frac{\bar{\lambda}_1}{\lambda_1}, \qquad \frac{C_{x_{i2}}}{\bar{C}_{x_{i1}}}=\left\{\frac{1+\frac{c_1}{2\bar{\lambda}_1}}{1+\frac{c_2}{2\lambda_2}}\right\}^2\left\{\frac{C_{z_{2\infty}}}{C_{z_{1\infty}}}\right\}^2\frac{\bar{\lambda}_1}{\lambda_1},$$

then the ratios of the lift and the induced drag of the aerofoil with discontinuities to those of the original aerofoil, $\mathfrak{L}$ and $\mathfrak{D}$, are

$$\mathfrak{L} = \frac{C_z}{\bar{C}_z} = \frac{1+\frac{c_1}{2\bar{\lambda}_1}}{1+\frac{c_1}{2\lambda_1}}(1-k)\Theta_1 + \frac{1+\frac{c_1}{2\bar{\lambda}_1}}{1+\frac{c_2}{2\lambda_2}}\cdot\frac{C_{z_{2\infty}}}{C_{z_{1\infty}}}k(1-\tau)\Theta_2, \quad \ldots\ldots \quad (64)$$

$$\mathfrak{D} = \frac{C_{x_i}}{\bar{C}_{x_i}} = \left\{\frac{1+\frac{c_1}{2\bar{\lambda}_1}}{1+\frac{c_1}{2\lambda_1}}\right\}^2\frac{\bar{\lambda}_1}{\lambda_1}(1-k)\Theta_3 + \left\{\frac{1+\frac{c_1}{2\bar{\lambda}_1}}{1+\frac{c_2}{2\lambda_2}}\right\}^2\left\{\frac{C_{z_{2\infty}}}{C_{z_{1\infty}}}\right\}^2\frac{\bar{\lambda}_1}{\lambda_1}k(1-\tau)\Theta_4,$$

$$\ldots\ldots\ldots\ldots\ldots\ldots\ldots\ldots\ldots\ldots\ldots\ldots\ldots\ldots \quad (65)$$

where

$$\Theta_1 = \left\{1+\frac{\frac{c_1}{2\lambda_1}}{1+\frac{c_1}{2\lambda_1}}\left(\frac{2}{\pi}I_1-1\right)+\frac{\frac{c_1}{2\lambda_1'}}{1+\frac{c_2}{2\lambda_2}}(1-\tau)\frac{c_{z_{2\infty}}}{c_{z_{1\infty}}}\left(\frac{2}{\pi}I_2-1\right)\right\}\Bigg/ \Bigg/\left\{1+\frac{\frac{c_1}{2\bar{\lambda}_1}}{1+\frac{c_1}{2\bar{\lambda}_1}}\left(\frac{2}{\pi}\bar{I}_1-1\right)\right\},$$

$$\Theta_2 = \left\{1+\frac{\frac{c_2}{\lambda_2'}}{1+\frac{c_1}{2\lambda_1}}\cdot\frac{1}{1-\tau}\cdot\frac{C_{z_{1\infty}}}{C_{z_{2\infty}}}\left(\frac{2}{\pi}I_3-1\right)\right\}\Bigg/\left\{1+\frac{\frac{c_1}{2\bar{\lambda}_1}}{1+\frac{c_1}{2\bar{\lambda}_1}}\left(\frac{2}{\pi}\bar{I}_1-1\right)\right\},$$

$$\Theta_3 = \left\{1-\left(\frac{2}{\pi}I_1-1\right)\left(1-\frac{\frac{c_1}{2\lambda_1}}{1+\frac{c_1}{2\lambda_1}}\right)\right.$$

$$\left.-\frac{\lambda_1}{\lambda_2}\cdot\frac{1+\frac{c_1}{2\lambda_1}}{1+\frac{c_2}{2\lambda_2}}\cdot\frac{C_{z_{2\infty}}}{C_{z_{1\infty}}}\left(\frac{2}{\pi}I_2-1\right)\left(1-\frac{2k}{1-k}\cdot\frac{\frac{c_1}{2\lambda_1'}}{1+\frac{c_1}{2\lambda_1}}\right)\right\}\Bigg/$$

$$\Bigg/2\left\{1-\frac{\bar{I}_1}{\pi}+\frac{\frac{c_1}{2\bar{\lambda}_1}}{1+\frac{c_1}{2\bar{\lambda}_1}}\left(\frac{\bar{I}_1}{\pi}-\frac{1}{2}\right)\right\},$$

$$\Theta_4 = \left\{ 1 - 2\frac{\lambda_2}{\lambda_1} \cdot \frac{1 + \frac{c_2}{2\lambda_2}}{1 + \frac{c_1}{2\lambda_1}} \cdot \frac{C_{z_{1\infty}}}{C_{z_{2\infty}}} \left(\frac{2}{\pi} I_3 - 1 \right) \left(1 - \frac{1-k}{2k} \cdot \frac{\frac{c_2}{2\lambda_2'}}{1 + \frac{c_2}{2\lambda_2}} \right) \right\} \Bigg/ 2 \left\{ 1 - \frac{\bar{I}_1}{\pi} + \frac{\frac{c_1}{2\bar{\lambda}_1}}{1 + \frac{c_1}{2\bar{\lambda}_1}} \left(\frac{\bar{I}_1}{\pi} - \frac{1}{2} \right) \right\}.$$

The calculation is compared with the experiment carried out with regard to the 75 cm × 15 cm aerofoil of Göttingen 593 section with the

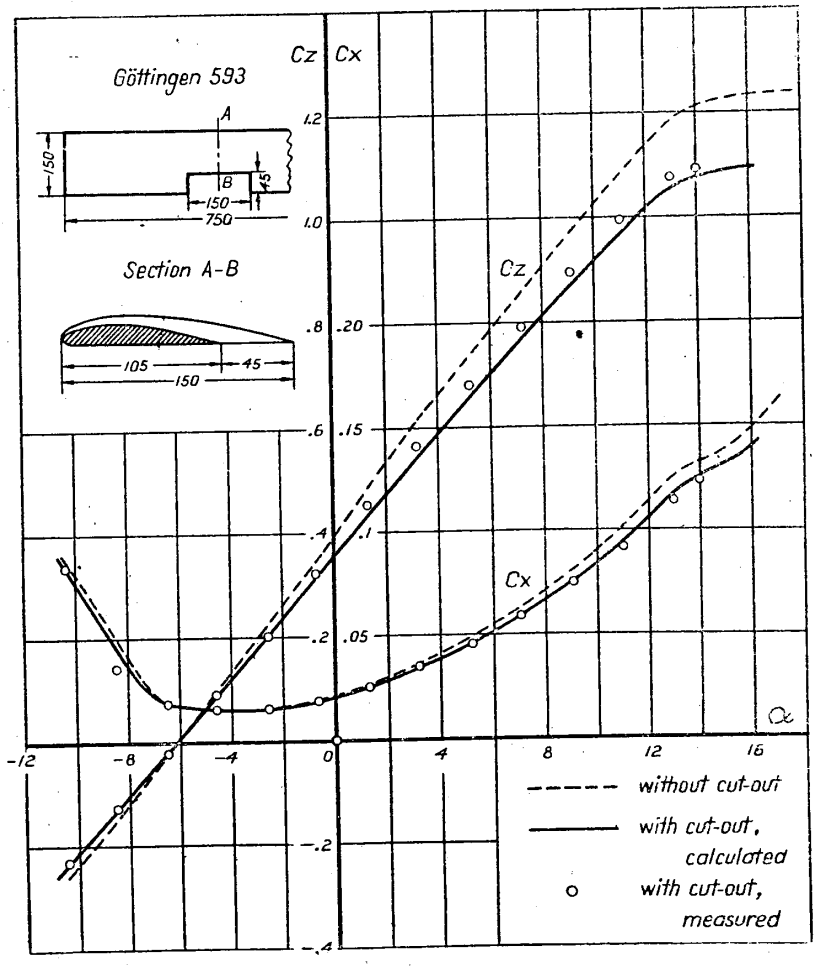

Fig. 15. Comparison of the calculation with the experiment.

rectangular cut-out of $k=0\cdot2$ and $\tau=0\cdot3$, in which $C_{z2\infty}/C_{z1\infty}=1$, $\lambda_1=2$, $\lambda_1'=1$, $\lambda_2=1\cdot4286$, $\lambda_2'=2\cdot8571$, $c_1=c_2=2\cdot5656$. The result of the calculation agrees comparatively well with the experimental result as shown in Fig. 15.

Part 3. Characteristics of Aerofoil with cut-out.

§3.1. *The slope of the lift curve of the aerofoil section.*

3.1.1. *The determination of the slope of the lift curve of the aerofoil section.*

The slope of the lift curve of the aerofoil section is usually determined from the data of the wind-tunnel test of the rectangular aerofoil by correcting the angle of incidence by the equation

$$\Delta\alpha = \frac{C_z}{\pi\lambda}(1+\tau)\,.$$

The value of τ in the above equation is dependent of both the aspect ratio and the slope of the lift curve, and hence the correction of the angle of incidence $\Delta\alpha$ can not exactly be predetermined. The usual method of the determination of the slope of the lift curve seems to be unsatisfactory and it is desirable to establish a proper method.

The distribution of circulation across the span of the rectangular aerofoil is expressed by the equation

$$\Gamma = \Gamma_\infty \sum A_n \sin n\theta\,.$$

In the above equation the variable θ is given by the relation $y=-b\cos\theta$ and Γ_∞ is the circulation in two-dimensional flow, which is expressed by $c_1 Vt\alpha$, where b is the semi-span, c_1 is $\frac{1}{2}(\partial C_z/\partial\alpha)_{\lambda\to\infty}$ or half the slope of the lift curve of the aerofoil section, V the velocity, t the chord length, α the angle of incidence.

If we determine the first four coefficients of the series by the following fundamental equation

$$\sum\left(1+\frac{c_1}{2\lambda}\cdot\frac{n}{\sin\theta}\right)A_n\sin n\theta = 1$$

so as to satisfy the conditions of the aerofoil shape at the four points $\theta = \pi/8, \pi/4, 3\pi/8$ and $\pi/2$, then we get

$$\left.\begin{aligned} A_1 &= \left[7{\cdot}1100+80{\cdot}7791\frac{c_1}{\lambda}+280.4106\left(\frac{c_1}{\lambda}\right)^2 \right.\\ &\qquad \left. +296{\cdot}9809\left(\frac{c_1}{\lambda}\right)^3\right]\cdot\frac{1}{D}, \\ A_3 &= \left[2{\cdot}1166+17{\cdot}2641\frac{c_1}{\lambda}+33{\cdot}4394\left(\frac{c_1}{\lambda}\right)^2\right]\cdot\frac{1}{D}, \\ A_5 &= \left[0{\cdot}9449+4{\cdot}4609\frac{c_1}{\lambda}+2{\cdot}6667\left(\frac{c_1}{\lambda}\right)^2\right]\cdot\frac{1}{D}, \\ A_7 &= \left[0{\cdot}2812+0{\cdot}6085\frac{c_1}{\lambda}+0{\cdot}3781\left(\frac{c_1}{\lambda}\right)^2\right]\cdot\frac{1}{D}, \end{aligned}\right\} \quad \cdots\cdots \quad (66)$$

where $$D = 5{\cdot}6571+69{\cdot}1255\frac{c_1}{\lambda}+272{\cdot}7756\left(\frac{c_1}{\lambda}\right)^2+392{\cdot}3704\left(\frac{c_1}{\lambda}\right)^3 +148{\cdot}4905\left(\frac{c_1}{\lambda}\right)^4.$$

The lift coefficient of the rectangular aerofoil becomes

$$C_z = \frac{\pi}{2}c_1\alpha A_1 \cdots\cdots\cdots\cdots\cdots\cdots \quad (67)$$

Now, denoting the lift coefficient for the aspect ratio λ_1 and λ_2 at a constant angle of incidence by $[C_z]_{\lambda_1}$ and $[C_z]_{\lambda_2}$, respectively, then we get from Eq. (67)

$$[C_z]_{\lambda_2} = [C_z]_{\lambda_1}\frac{[A_1]_{\lambda_2}}{[A_1]_{\lambda_1}}.$$

Differentiating this by α, we get

$$\left[\frac{\partial C_z}{\partial\alpha}\right]_{\lambda_2} = \left[\frac{\partial C_z}{\partial\alpha}\right]_{\lambda_1}\cdot\frac{[A_1]_{\lambda_2}}{[A_1]_{\lambda_1}} \cdots\cdots\cdots\cdots\cdots \quad (68)$$

If we take $\lambda_2 = \infty$ and write $\left[\frac{\partial C_z}{\partial \alpha}\right]_{\lambda_2 \to \infty} = \frac{\partial C_{z\infty}}{\partial \alpha} = 2c_1$ and $\left[\frac{\partial C_z}{\partial \alpha}\right]_{\lambda_1} = 2c_1'$, then we get from Eq. (68)

$$c_1 = c_1' \frac{1 \cdot 2568}{[A_1]_{\lambda_1}}.$$

Substituting the equation (66) into the above equation, we get

$$\frac{c_1\left[7 \cdot 1100 + 80 \cdot 7791\frac{c_1}{\lambda_1} + 280.4106\left(\frac{c_1}{\lambda_1}\right)^2 + 296 \cdot 9809\left(\frac{c_1}{\lambda_1}\right)^3\right]}{5 \cdot 6571 + 69 \cdot 1255\frac{c_1}{\lambda_1} + 272 \cdot 7756\left(\frac{c_1}{\lambda}\right)^2 + 392 \cdot 3704\left(\frac{c_1}{\lambda}\right)^3 + 148 \cdot 4905\left(\frac{c_1}{\lambda}\right)^4}$$

$$= 1 \cdot 2568 c_1' \quad \ldots\ldots\ldots\ldots\ldots\ldots\ldots\ldots\ldots\ldots\ldots\ldots \quad (69)$$

The relation between c_1 and c_1' expressed by the above equation is shown in Fig. 16. If we obtain the slope of the lift curve of an aerofoil of a given

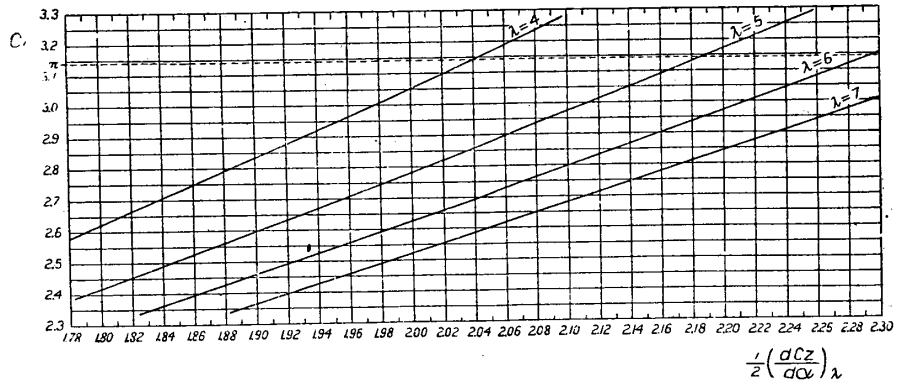

Fig. 16. The relation between half the slope of the lift curve of the aerofoil section and that of the aerofoil of finite aspect ratio ($\lambda = 4$, 5, 6 and 7).

aspect ratio, $2c_1'$, from the result of the wind-tunnel test, then we can immediately find the value of $\partial C_{z\infty}/\partial \alpha$ corresponding to that aerofoil section from the curves shown in Fig. 16.

The slope of the lift curve of the aerofoil section, whose trailing edge is cut away, obtained by the above method is shown in Fig. 17.

It is found that the value of $\partial C_{z\infty}/\partial\alpha$ increases considerably as the depth of cut-out increases and the rate of increase is independent of the aerofoil section.

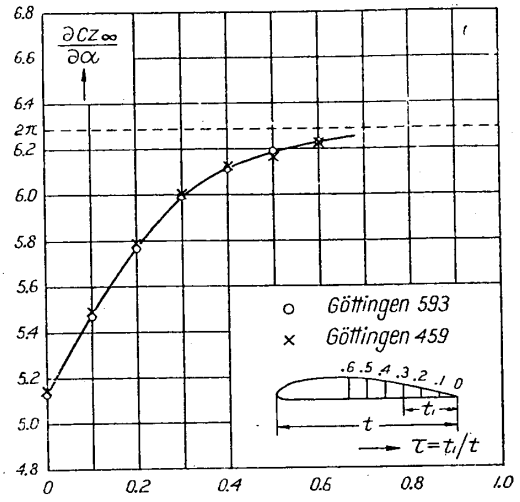

Fig. 17. The values of $\partial c_{z\infty}/\partial\alpha$ of the aerofoil section whose trailing edge is cut away.

For the purpose of finding the value of $\partial C_{z\infty}/\partial\alpha$ of the commonly used aerofoil we analyse the results of one hundred and twenty aerofoils tested at Göttingen 2·26 m tunnel (Reference 3), R.A.E. No. 1 Tunnel (Reference 4), N. A. C. A. Variable-Density tunnel (Reference 5), C.A.H.I. T-1 tunnel (Reference 6), Eiffel tunnel (Reference 7) and A.R.I. Tokyo Imp. Univ. 1·5 m tunnel. The results of the analysis are shown as the function of

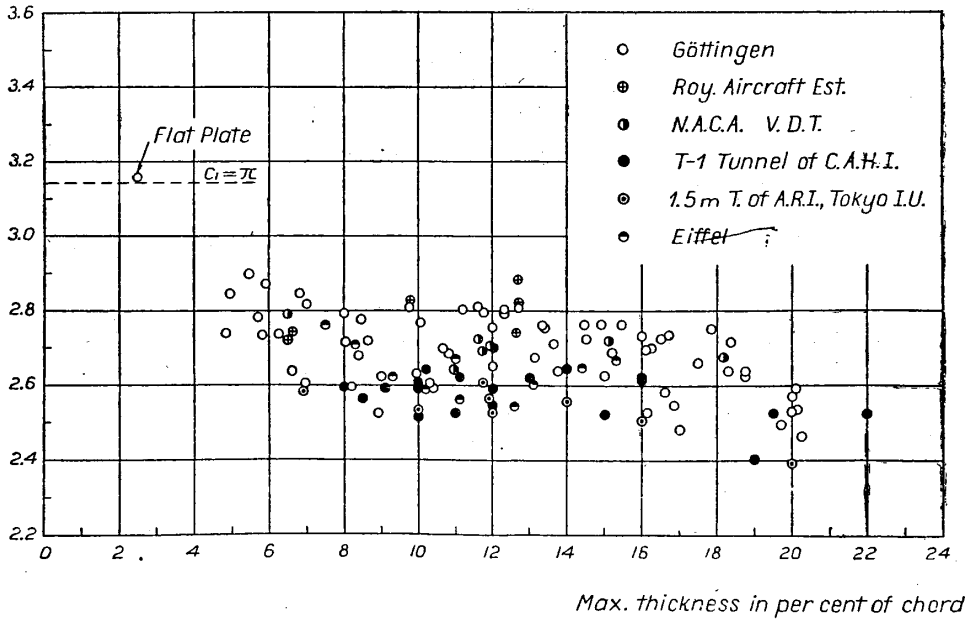

Fig. 18. The variation of the values of c_1 of the aerofoils with the thickness ratio.

the thickness ratio in Fig. 18. It is shown that the value of $\partial C_{z\infty}/\partial a$ decreases as the thickness ratio increases.

If we compare the results from the various wind-tunnels with regard to the mean values of $\partial C_{z\infty}/\partial a$ taken in the range of thickness ratio from 0·10 to 0·14, then it is found that the value of c_1 varies with the wind-tunnel as shown in Table 4, and this variation is considered to be

TABLE 4.

Wind-tunnel	Test Reynolds number	Critical Reynolds number	c_1	$\sigma=\frac{c_1}{\pi}$
Göttingen 2·26 m T.	$0{\cdot}4\times10^6$	$3{\cdot}2\times10^5$	2·7137	0·864
R. A. E. No. 1 T.	$0{\cdot}2\times10^6$	$1{\cdot}9\times10^5$	2·7899	0·888
N. A. C. A. V. D. T.	$3{\cdot}7\times10^6$	$1{\cdot}6\times10^5$	2·7077	0·862
C. A. H. I. T-1	$0{\cdot}6\sim1{\cdot}0\times10^6$	$3{\cdot}0\times10^5$	2·5872	0·824
Eiffel	$0{\cdot}3\times10^6$	$1{\cdot}4\times10^5$	2·6379	0·840
A.R.I. Tokyo, 1·5 m T.	$0{\cdot}3\sim0{\cdot}4\times10^6$	$3{\cdot}6\times10^5$	2·5543	0·813

due to the differences in the test Reynolds number, the turbulence of the air stream and the static pressure gradient in the direction of the air stream. Silverstein's experiment (Reference 8) shows that the value of c_1 increases as the test Reynolds number increases and Millikan-Klein's experiment (Reference 9) shows that it increases as the turbulence of the air stream increases. Table 4, however, shows that the result from the wind-tunnel of large test Reynolds number and of much turbulence does not always give the large value of c_1, and hence the effect of the gradient of the static pressure is supposed to be of importance.

3.1.2. *The effect of the pressure gradient on the slope of the lift curve.*

We restrict the motion to the two-dimensional. If we suppose a source of strength m at the point $x=-r_1$ behind the body as shown in Fig. 19, then the velocity on the x-axis becomes

$$u = -V + \frac{m}{2\pi} \cdot \frac{1}{r_1 + x}$$

and the velocity gradient is

$$\frac{du}{dx} = -\frac{m}{2\pi} \cdot \frac{1}{(r_1+x)^2} \qquad (70)$$

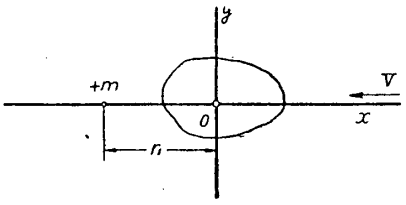

Fig. 19.

The relation between the velocity gradient and the pressure gradient is from Bernonlli's theorem

$$\frac{dp}{dx} + \rho u \frac{du}{dx} = 0 \quad \ldots\ldots\ldots\ldots\ldots\ldots \quad (71)$$

Therefore, the pressure gradient at the origin becomes

$$\frac{dp}{dx} = \rho\left(-V + \frac{m}{2\pi r_1}\right)\frac{m}{2\pi r_1^2} \quad \ldots\ldots\ldots\ldots \quad (72)$$

If we choose r_1 sufficiently large, the above equation becomes approximately

$$\frac{dp}{dx} = -\frac{\rho V m}{2\pi r_1^2} \quad \ldots\ldots\ldots\ldots\ldots\ldots \quad (72a)$$

Hence if the pressure gradient at the origin is known, we can determine the strength of source by the above equation.

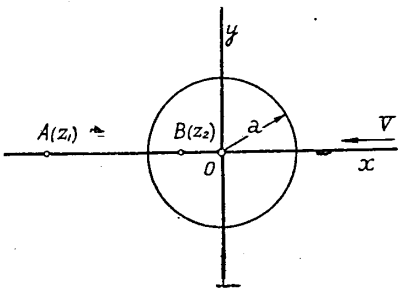

Fig. 20.

Consider the flow around the circular cylinder of radius a placed in the stream with the pressure gradient which is produced by a source of strength m at the point $z_1 = -r_1$ as shown in Fig. 20. Then, the potential function becomes

$$w = -V\left(z + \frac{a^2}{z}\right) - \frac{i\Gamma}{2\pi}\log\frac{z}{a} + \frac{m}{2\pi}\log\frac{(z-z_1)(z-z_2)}{z}, \quad \ldots \quad (73)$$

where z_2 is the inverse point of z_1 with regard to the circle, and the complex velocity is

$$\frac{dw}{dz} = \bar{v} = v_x - iv_y = -V\left(1-\frac{a^2}{z^2}\right) - \frac{i\Gamma}{2\pi}\cdot\frac{1}{z} + \frac{m}{2\pi}\left(\frac{1}{z-z_1}+\frac{1}{z-z_2}-\frac{1}{z}\right) \quad \cdots\cdots (74)$$

The force acting the cylinder can be calculated by Lagally's equation (Reference 10)

$$P_x - iP_y = \frac{1}{2}i\rho\int_C\left(\frac{dw}{dz}\right)^2 dz + \rho\int_R\left(\frac{dw}{dz}\right)\nabla\mathfrak{v}\,d\sigma - i\rho\int_R\left(\frac{dw}{dz}\right)|\,rot\,\mathfrak{v}\,|\,d\sigma\,, \quad \cdots\cdots (75)$$

where P_x and P_y are the x- and y-component of the force respectively, the contour C is a large closed curve taken round the cylinder, R the space between the surface of the cylinder and the contour C, and $d\sigma$ the elementary area of this space.

The velocity at the point A omitting the source at the point A in the calculation, $\bar{v}_A^*$ say, is

$$\bar{v}_A^* = -V\left(1-\frac{a^2}{r_1^2}\right) + \frac{i\Gamma}{2\pi r_1} - \frac{m}{2\pi}\cdot\frac{a^2}{r_1(r_1^2-a^2)} \quad \cdots\cdots (76)$$

Then, the force acting the cylinder is from (75)

$$P_x - iP_y = \rho(m-i\Gamma)V + \rho m\bar{v}_A^*\,.$$

Therefore

$$\left.\begin{aligned} P_x &= \rho m V\frac{a^2}{r_1^2} - \frac{\rho m^2}{2\pi}\cdot\frac{a^2}{r_1(r_1^2-a^2)}\,, \\ P_y &= \rho V\Gamma - \frac{\rho m\Gamma}{2\pi r_1}\,. \end{aligned}\right\} \quad \cdots\cdots (77)$$

The strength of source for a given pressure gradient is determined by (72a).

$$m = -\frac{2\pi r_1^2}{\rho V}\cdot\frac{dp}{dx}\,.$$

Hence, the lift L and the drag D of the cylinder are

$$\left.\begin{aligned} L &= P_y = \rho V\Gamma + \frac{r_1\Gamma}{V}\cdot\frac{dp}{dx}\,, \\ D &= -P_x = 2\pi a^2\frac{dp}{dx} + \frac{a^2}{r_1^2-a^2}\cdot\frac{2\pi r_1^3}{\rho V^2}\left(\frac{dp}{dx}\right)^2. \end{aligned}\right\} \quad \cdots\cdots \quad (78)$$

It follows that when $\frac{dp}{dx}<0$ or the increasing pressure gradient exists the lift and drag decrease and when $\frac{dp}{dx}>0$ or the decreasing pressure gradient exists the lift and drag increase.

Secondly, consider the flat plate placed with the angle of incidence α in the stream with the pressure gradient. The flow around the flat plate is obtained from the flow around the circular cylinder shown in Fig. 21 by the conformal transformation $\xi = z + \frac{a^2}{z}$.

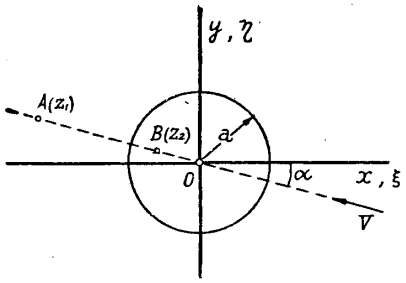

Fig. 21.

The potential function of the flow around this circular cylinder is

$$w = -V\left(ze^{i\alpha} + \frac{a^2e^{-i\alpha}}{z}\right) - \frac{i\Gamma}{2\pi}\log\frac{z}{a} + \frac{m}{2\pi}\log\frac{(z-z_1)(z-z_2)}{z}, \quad (79)$$

where $z_1 = -r_1e^{-i\alpha}$ and $z_2 = -r_2e^{-i\alpha} = -\frac{a^2}{r_1}e^{-i\alpha}$. The velocity of the flow around the flat plate becomes

$$\frac{dw}{d\zeta} = v_\xi - iv_\eta = \left\{-V\left(e^{i\alpha} - \frac{a^2e^{-i\alpha}}{z^2}\right) - \frac{i\Gamma}{2\pi}\cdot\frac{1}{z} + \frac{m}{2\pi}\left(\frac{1}{z-z_1} + \frac{1}{z-z_2} - \frac{1}{z}\right)\right\}\cdot\frac{z^2}{z^2-a^2} \cdots\cdots \quad (80)$$

Denoting the velocity at the point A omitting the source at A in the calculation by $\bar{v}_A^*$, then we get from (75)

$$P_\xi - iP_\eta = \rho(m - i\Gamma)Ve^{i\alpha} + \rho m\bar{v}_A^* \cdots\cdots\cdots \quad (81)$$

Writing $\bar{v}_A^* = v_{\xi A}^* - iv_{\eta A}^*$, then we get

$$\left.\begin{aligned} P_\xi &= \rho V\Gamma \sin\alpha + \rho m V\cos\alpha + \rho m v_{\xi A}^* , \\ P_\eta &= \rho V\Gamma\cos\alpha - \rho m V\sin\alpha + \rho m v_{\eta A}^* . \end{aligned}\right\} \cdots\cdots\cdots \quad (82)$$

The lift and drag are

$$L = P_\eta\cos\alpha + P_\xi\sin\alpha ,$$

$$D = P_\eta\sin\alpha - P_\xi\cos\alpha ,$$

and it follows that

$$\left.\begin{aligned} L &= \rho V\Gamma + \rho m(v_{\eta A}^*\cos\alpha + v_{\xi A}^*\sin\alpha) , \\ D &= -\rho m V + \rho m(v_{\eta A}^*\sin\alpha - v_{\xi A}^*\cos\alpha) . \end{aligned}\right\} \cdots\cdots \quad (83)$$

If we determine the circulation so that the flow may leave smoothly from the trailing edge, we get

$$\Gamma = 4\pi aV\sin\alpha - \frac{2amr_1\sin\alpha}{a^2 - 2ar_1\cos\alpha + r_1^2} \cdots\cdots\cdots \quad (84)$$

Assuming that the angle of incidence is small and the distance of the source is large compared with the chord length, then we can neglect the small quantities α^2 and $\frac{a^2}{r_1^2}\alpha$. Hence, the velocities $v_{\xi A}^*$ and $v_{\eta A}^*$ are from (80)

$$\left.\begin{aligned} v_{\xi A}^* &= \left\{-V + V\frac{a^2}{r_1^2} - \frac{ma^2}{2\pi r_1(r_1^2 - a^2)} - \frac{\Gamma\alpha}{2\pi r_1}\right\}\frac{r_1^2}{r_1^2 - a^2} \\ v_{\eta A}^* &= -\left\{-V\alpha + V\alpha\frac{a^2}{r_1^2} - \frac{ma^2\alpha}{2\pi r_1(r_1^2 - a^2)} + \frac{\Gamma}{2\pi r_1}\right\}\frac{r_1^2}{r_1^2 - a^2} \end{aligned}\right\} \quad (85)$$

and the circulation becomes

$$\Gamma = 4\pi a V\alpha - \frac{2amr_1\alpha}{(r_1-a)^2} \cdots\cdots\cdots\cdots \quad (86)$$

The lift and drag are

$$L = \rho V\Gamma + \rho m(v^*_{\eta A} + \alpha v^*_{\xi A}) ,$$

$$D = -\rho mV - \rho m(v^*_{\xi A} - \alpha v^*_{\eta A}) .$$

Substituting (85) and (86) into the above equations, we get

$$\left.\begin{aligned} L &= 4\pi a\rho V^2\alpha - 4a\rho Vm\alpha\frac{r_1^2}{(r_1^2-a^2)(r_1-a)} \\ &\qquad + \frac{a\rho m^2\alpha}{\pi}\cdot\frac{r_1^2}{(r_1^2-a^2)(r_1-a)^2} , \\ D &= -\rho mV - \rho m\left\{-V + V\frac{a^2}{r_1^2} - \frac{m}{2\pi}\cdot\frac{a^2}{r_1(r_1^2-a^2)}\right\}\frac{r_1^2}{r_1^2-a^2} . \end{aligned}\right\} \quad (87)$$

It follows that when $m>0$ or the increasing pressure gradient exists the lift and drag decrease and when $m<0$ or the decreasing pressure gradient exists the lift and drag increase.

If we obtain the lift coefficient C_z and differentiate it with regard to α, then we get

$$\frac{\partial C_z}{\partial\alpha} = 2\pi - 2\left(\frac{m}{V}\right)\frac{r_1^2}{(r_1^2-a^2)(r_1-a)} + \frac{1}{2\pi}\left(\frac{m}{V}\right)^2\frac{r_1^2}{(r_1^2-a^2)(r_1-a)^2} \quad (88)$$

If follows that when the increasing pressure gradient exists the slope of the lift curve decreases and when the decreasing pressure gradient exists it increases.

§3.2. *General equations for calculating the lift distribution.*

In many usual calculations it has been assumed that the slope of the lift curve of the aerofoil section is constant along the span, but in the case of the aerofoil with cut-out the slope of the lift curve of the wing section must be considered to vary along the span because the slope of the lift curve of the section, whose trailing edge is cut away, increases considerably as seen in Fig. 17.

If we express the distribution of circulation by the following series

$$\Gamma = c_{10} V t_0 \alpha_0 \sum_{n=1}^{\infty} A_n \sin n\theta , \quad \cdots\cdots\cdots\cdots \quad (89)$$

where c_{10}, t_0 and α_0 are half the slope of the lift curve, the chord length and the geometrical angle of incidence at the basic point of the aerofoil respectively, then the fundamental equation (5) becomes

$$\frac{t_0}{t_{(y)}} \sin\theta \sum A_n \sin n\theta + \frac{c_{10} t_0}{4b} \cdot \frac{c_{1(y)}}{c_{10}} \sum n A_n \sin n\theta = \frac{c_{1(y)}}{c_{10}} \cdot \frac{\alpha_{(y)}}{\alpha_0} \sin\theta \cdots\cdots \quad (90)$$

Write

$$p = \frac{c_{10} t_0}{4b} , \quad \cdots\cdots\cdots\cdots\cdots \quad (91)$$

$$\left.\begin{aligned} \frac{\alpha_{(y)}}{\alpha_0} \sin\theta &= \sum B_n \sin n\theta , \\ \frac{t_0}{t_{(y)}} \sin\theta &= \sum C_{2n} \cos 2n\theta , \\ \frac{c_{1(y)}}{c_{10}} &= \sum D_{2n} \cos 2n\theta . \end{aligned}\right\} \quad \cdots\cdots\cdots\cdots \quad (92)$$

Then we get the following equations from the equation (90)

$$
\left.\begin{aligned}
&A_1\left\{\left(C_0-\frac{1}{2}C_2\right)+p\left(D_0-\frac{1}{2}D_2\right)\right\}\\
&\quad=\beta_1-\left[\frac{A_3}{2}\left\{(C_2-C_4)+3p(D_2-D_4)\right\}\right.\\
&\qquad\left.+\frac{A_5}{2}\left\{(C_4-C_6)+5p(D_4-D_6)\right\}+\cdots\right],\\
&A_2\left\{\left(C_0-\frac{1}{2}C_4\right)+2p\left(D_0-\frac{1}{2}D_4\right)\right\}\\
&\quad=\beta_2-\left[\frac{A_4}{2}\left\{(C_2-C_6)+4p(D_2-D_6)\right\}\right.\\
&\qquad\left.+\frac{A_6}{2}\left\{(C_4-C_8)+6p(D_4-D_8)\right\}+\cdots\right],\\
&A_3\left\{\left(C_0-\frac{1}{2}C_6\right)+3p\left(D_0-\frac{1}{2}D_6\right)\right\}\\
&\quad=\beta_3-\frac{A_1}{2}\left\{(C_2-C_4)+p(D_2-D_4)\right\}\\
&\qquad-\left[\frac{A_5}{2}\left\{(C_2-C_8)+5p(D_2-D_8)\right\}+\cdots\right],\\
&\quad\cdots\cdots\cdots\\
&A_n\left\{\left(C_0-\frac{1}{2}C_{2n}\right)+np\left(D_0-\frac{1}{2}D_{2n}\right)\right\}\\
&\quad=\beta_n-\frac{A_{n-2}}{2}\left\{\left(C_2-\frac{1}{2}C_{2n-2}\right)+(n-2)p\left(D_2-\frac{1}{2}D_{2n-2}\right)\right\}\\
&\qquad-\frac{A_{n-4}}{2}\left\{\left(C_4-\frac{1}{2}C_{2n-4}\right)+(n-4)p\left(D_4-\frac{1}{2}D_{2n-4}\right)\right\}\\
&\qquad-\cdots\cdots-\frac{A_1}{2}\left\{(C_{n-1}-C_{n+1})+p(D_{n-1}-D_{n+1})\right\}\\
&\qquad-\left[\frac{A_{n+2}}{2}\left\{(C_2-C_{2n+2})+(n+2)p(D_2-D_{2n+2})\right\}\right.\\
&\qquad\left.+\frac{A_{n+4}}{2}\left\{(C_4-C_{2n+4})+(n+4)p(D_4-D_{2n+4})\right\}+\cdots\right],
\end{aligned}\right\}\qquad(93)
$$

where

$$\beta_1 = B_1\left(D_0-\frac{1}{2}D_2\right)+\left[\frac{B_3}{2}(D_2-D_4)+\frac{B_5}{2}(D_4-D_6)+\frac{B_7}{2}(D_6-D_8)+\cdots\right]$$

$$\beta_2 = B_2\left(D_0-\frac{1}{2}D_4\right)+\left[\frac{B_4}{2}(D_2-D_6)+\frac{B_6}{2}(D_4-D_8)+\frac{B_8}{2}(D_6-D_{10})+\cdots\right]$$

$$\beta_3 = B_3\left(D_0-\frac{1}{2}D_6\right)+\frac{B_1}{2}(D_2-D_4)+\left[\frac{B_5}{2}(D_2-D_8)+\frac{B_7}{2}(D_4-D_{10})+\cdots\right]$$

$$\cdots\cdots\cdots$$

$$\beta_n = B_n\left(D_0-\frac{1}{2}D_{2n}\right)+\frac{B_{n-2}}{2}(D_2-D_{2n-2})+\frac{B_{n-4}}{2}(D_4-D_{2n-4})+\cdots$$

$$+\frac{B_1}{2}(D_{n-1}-D_{n+1})$$

$$+\left[\frac{B_{n+2}}{2}(D_2-D_{2n+2})+\frac{B_{n+4}}{2}(D_4-D_{2n+4})+\cdots\right]$$

If the plan form of the aerofoil is given or the coefficients B_n, C_{2n} and D_{2n} are given, then the coefficients A_n are determined by the above equations. As a special case, if the slope of the lift curve of the aerofoil section is constant along the span, then $D_0 = 1$, $D_2 = D_4 = \cdots = 0$ and we obtain Lotz's formula (Reference 11).

The lift and the induced drag are

$$L = \frac{1}{2}\pi c_{10}\rho V^2 b t_0 \alpha_0 A_1 \quad \cdots\cdots\cdots\cdots\cdots\cdots \quad (94)$$

$$D_i = \frac{L^2}{2\pi b^2 \rho V^2}\cdot\frac{\sum nA_n^2}{A_1^2} \quad \cdots\cdots\cdots\cdots\cdots \quad (95)$$

Write

$$1+\delta = \frac{\sum nA_n^2}{A_1^2} \quad \cdots\cdots\cdots\cdots\cdots\cdots\cdots \quad (96)$$

Then, the lift coefficient and the induced drag coefficient are

$$C_z = \frac{1}{2}\pi c_{10}\frac{t_0}{t_m}\alpha_0 A_1 \quad \cdots\cdots\cdots\cdots\cdots\cdots \quad (97)$$

$$C_{x_i} = \frac{C_z^2}{\pi\lambda}(1+\delta), \quad \cdots\cdots\cdots\cdots\cdots\cdots \quad (98)$$

where $t_m = \frac{S}{2b}$ the mean chord length, S the wing area, and $\lambda = \frac{b^2}{S}$ the aspect ratio.

§3.3. *The characteristics of the aerofoil with rectangular cut-out in which the geometrical angle of incidence and $\partial C_{z\infty}/\partial\alpha$ are constant and the chord length varies discontinuously along the span.*

We calculate the lift distribution of the aerofoil with rectangular cut-out, whose cutaway section is similar to the original section, where the aspect ratio of the original aerofoil is 5 and the basic point of the aerofoil is taken at the centre of the original aerofoil. The calculation is carried out for the cases in which the depth of cut-out is varied in $\tau = 0{\cdot}3$ and, 0·6 and the width of cut-out is varied in $k = 0{\cdot}195$, 0·419, 0·619, 0·832, 1·000 for each depth, where k is the ratio of the width of cut-out to the span and τ the ratio of the depth of cut-out to the chord length. In this case $\alpha_0 = \alpha_{(y)}$ and $c_{10} = c_{1(y)} = 0{\cdot}85\pi$. Hence ti follows that $B_1 = 1$, $B_3 = B_5 = \cdots = 0$ and $D_0 = 1$, $D_2 = D_4 = \cdots = 0$. The coefficients C_{2n} are determined such that the boundary conditions of the aerofoil shape may be satisfied at the twenty points $\theta = \pi/40$, $2\pi/40$, $3\pi/40 \cdots \pi/2$ along the span. The chord distribution expressed by the Fourier series, taking the first twenty terms, is compared with the actual distribution in Fig. 23. It is seen that the difference between the assumed distribution and the actual distribution becomes remarkable as the depth of cut-out increase.

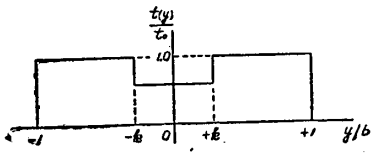

Fig. 22.

The coefficients A_n of the series expressing the circulation are tabulated in Table 5, and the calculated distributions of circulation are shown in Fig. 24 and 25.

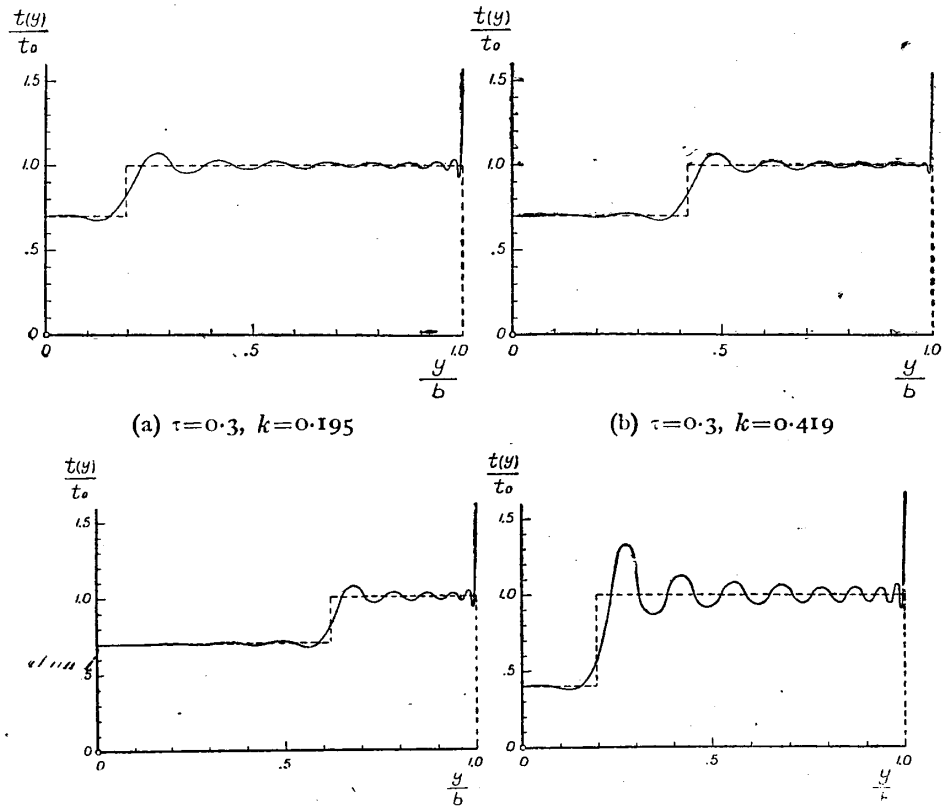

(a) $\tau=0.3$, $k=0.195$ (b) $\tau=0.3$, $k=0.419$

(c) $\tau=0.3$ $k=0.619$ (d) $\tau=0.6$, $k=0.195$

Fig. 23. Comparison of the chord distribution expressed by the Fourier series (full line) and the actual distribution (dotted line).

TABLE 5. The values of A_n.

	$\tau=0$	$\tau=0.3$					$\tau=0.6$				
	$k=0$	$k=.195$	$k=.419$	$k=.619$	$k=.832$	$k=1.\infty$	$k=.195$	$k=.419$	$k=.619$	$k=.832$	$k=1.\infty$
A_1	+.9140	+.8544	+.7951	+.7477	+.7079	+.6935	+.7679	+.6414	+.5431	+.4623	+.4337
A_3	+.1101	+.1470	+.1681	+.1602	+.1252	+.1013	+.2003	+.2408	+.2167	+.1334	+.0810
A_5	+.0233	−.0032	−.0010	+.0258	+.0398	+.0247	−.0412	−.0296	+.0345	+.0615	+.0246
A_7	+.0067	+.0248	+.0085	−.0078	+.0100	+.0077	+.0502	+.0074	−.0276	+.0168	+.0089
A_9	+.0024	−.0094	+.0099	+.0052	−.0018	+.0029	−.0259	+.0221	+.0070	−.0062	+.0037
A_{11}	+.0011	+.0085	−.0069	+.0068	−.0030	+.0013	+.0174	−.0181	+.0156	−.0066	+.0017
A_{13}	+.0005	+.0020	+.0042	−.0029	+.0002	+.0007	−.0069	+.0084	−.0071	−.0005	+.0009
A_{15}	+.0003	+.0021	+.0013	−.0018	+.0024	+.0004	+.0010	+.0038	−.0057	+.0053	+.0005
A_{17}	+.0002	+.0012	−.0032	+.0031	+.0017	+.0002	+.0038	−.0086	+.0072	+.0042	+.0003
A_{19}	+.0001	−.0020	+.0031	+.0005	−.0002	+.0001	−.0065	+.0073	+.0020	−.0004	+.0002

Denoting the induced angle of incidence by α_i, then we get

$$\frac{\alpha_i}{\alpha} = \frac{w}{V\alpha} = \frac{c_{10}t_0}{4b}\sum nA_n\frac{\sin n\theta}{\sin\theta},$$

$$\frac{\Gamma_{(y)}}{\Gamma_\infty} = \frac{C_{z(y)}}{C_{z\infty}}\cdot\frac{t_{(y)}}{t_0},$$

and hence

$$\frac{C_{z(y)}}{C_{z\infty}} = \frac{\Gamma_{(y)}}{\Gamma_\infty}\cdot\frac{t_0}{t_{(y)}} = \frac{\alpha_e}{\alpha} = 1-\frac{w}{V\alpha}.$$

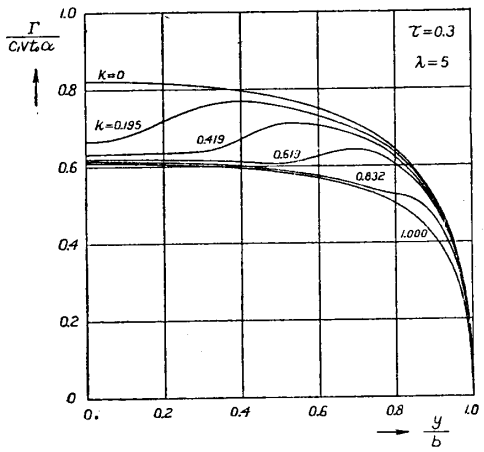

Fig. 24. The distribution of circulation along the span. (The depth of cut-out, $\tau=0\cdot3$).

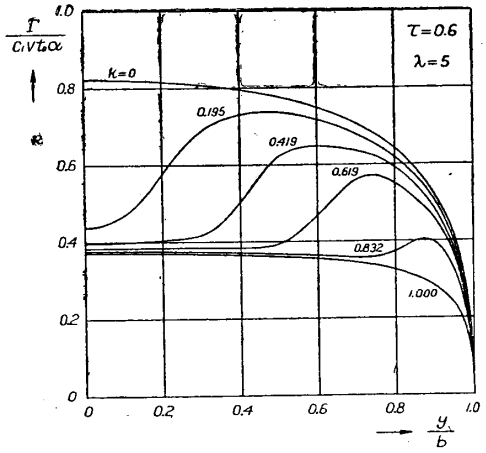

Fig. 25. The distribution of circulation along the span. (The depth of cut-out, $\tau=0\cdot6$).

The distributions of the induced velocity $w_{(y)}$, the effective angle of incidence $\alpha_{e(y)}$ and the lift coefficient of the section $Cz_{(y)}$ are shown in Figs. 26 and 27. In the case in which the wing section is uniform along the span it may be supposed that the stall begins at the point where the maximum of the distribution of the lift coefficient of the section occurs. Hence, it is supposed from the above figures that the stall begins at the corner of the cutaway portion and it extends towards the centre.

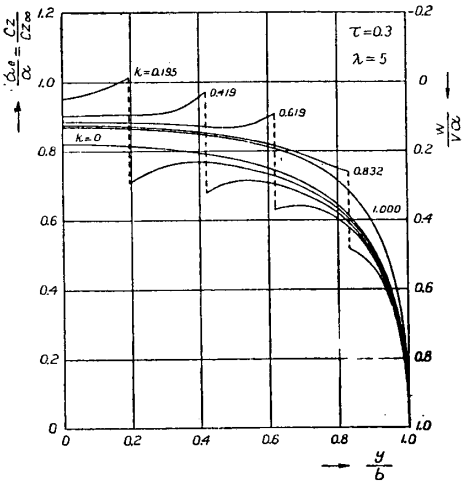

Fig. 26. The distributions of the induced velocity, the effective angle of incidence and the lift coefficient along the span. (The depth of cut-out, $\tau=0{\cdot}3$).

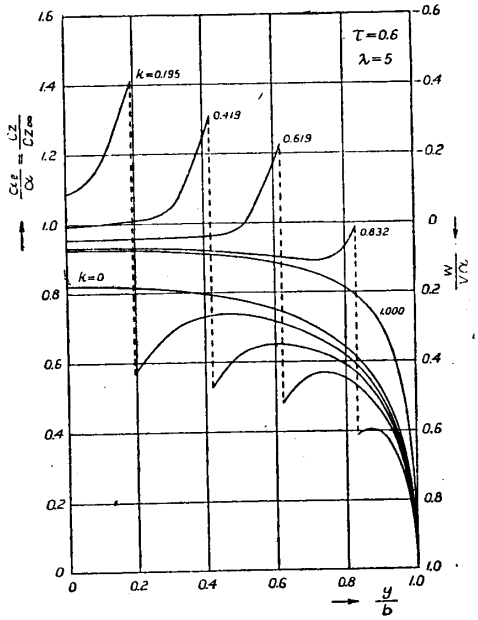

Fig. 27. The distributions of the induced velocity, the effective angle of incidence and the lift coefficient along the span. (The depth of cut-out, $\tau=0{\cdot}6$).

The distribution of the induced drag is given by the equation

$$\frac{dD_i}{dy} = \frac{1}{2}\rho V^2 t_0 C_{z\infty}^2 \cdot \frac{1}{2c_1} \cdot \frac{\Gamma}{\Gamma_\infty} \cdot \frac{\alpha_i}{\alpha},$$

and it is shown in Figs. 28 and 29. The induced drag of the cutaway portion is very small and it becomes negative when the depth of cut-out is considerably large.

The ratio of the lift of the aerofoil with cut-out L to that of the original aerofoil $\bar{L}$ at the given angle of incidence is

$$\mathfrak{L} = \frac{L}{\bar{L}} = \frac{A_1 \text{ cut-out}}{A_1 \text{ original}}$$

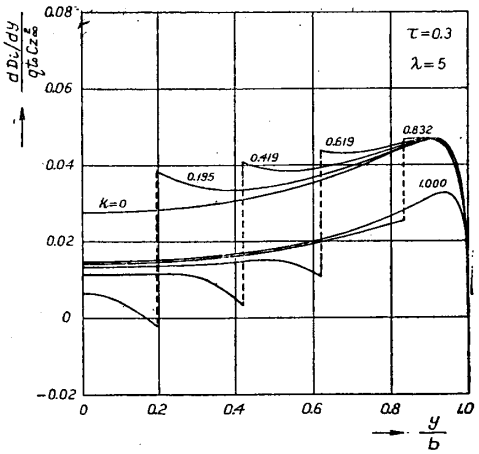

Fig. 28. The distribution of the induced drag along the span. (The depth of cut-out, $\tau=0{\cdot}3$).

whose values are shown in Table 6 and in Figs. 30 and 31.

The ratio of the induced drag of the aerofoil with cut-out D_i to that of the original aerofoil $\bar{D}_i$ is

$$\mathfrak{D} = \frac{D_i}{\bar{D}_i} = \frac{[\sum nA_n^2]\,\text{cut-out}}{[\sum nA_n^2]\,\text{original}}$$

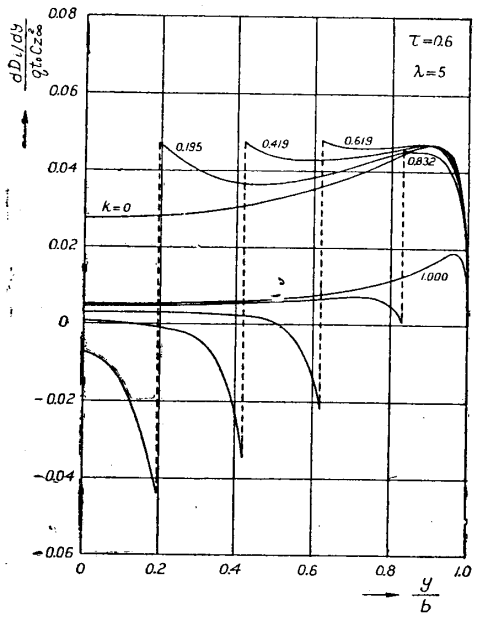

Fig. 29. The distribution of the induced drag the span. (The depth of cut-out, $\tau=0.6$).

whose values are shown in Table 6 and in Figs. 32 and 33. The values of δ in the equation of the induced drag coefficient are shown

TABLE 6. The values of $\mathfrak{L}$, $\mathfrak{D}$ and δ

	$\tau=0$	$\tau=0.3$					$\tau=0.6$				
	$k=0$	$k=.195$	$k=.419$	$k=.619$	$k=.832$	$k=1.000$	$k=.195$	$k=.419$	$k=.619$	$k=.832$	$k=1.000$
$\mathfrak{L}$	1.0000	.9348	.8699	.8181	.7745	.7588	.8402	.7018	.5942	.5058	.4745
$\mathfrak{D}$	1.0000	.9155	.8224	.7325	.6367	.5890	.8539	.6873	.5168	.3310	.2417
δ	.0473	.0972	.1381	.1464	.1116	.0714	.2669	.4617	.5329	.3549	.1244

in Table 6 and Fig. 34. The maximum value of δ occurs at nearly $k = 0{\cdot}55$.

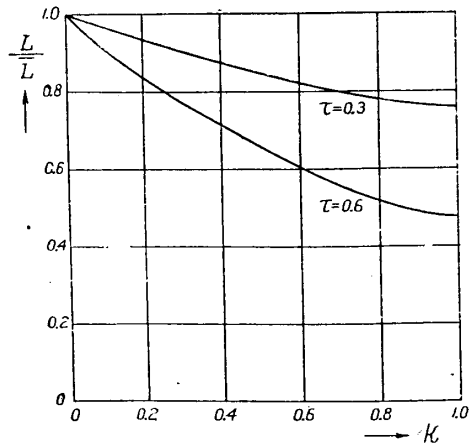

Fig. 30. The variation of the lift ratio $L/\bar{L}$ with the width of cut-out.

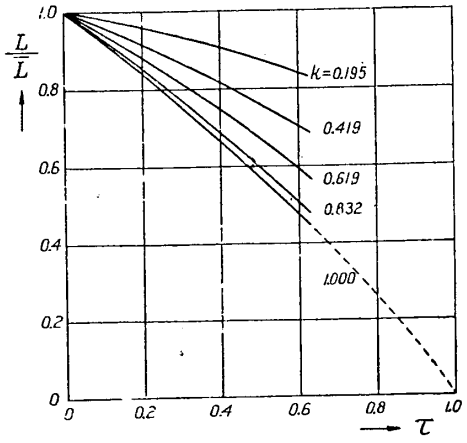

Fig. 31. The variation of the lift ratio $L/\bar{L}$ with the depth of cut-out.

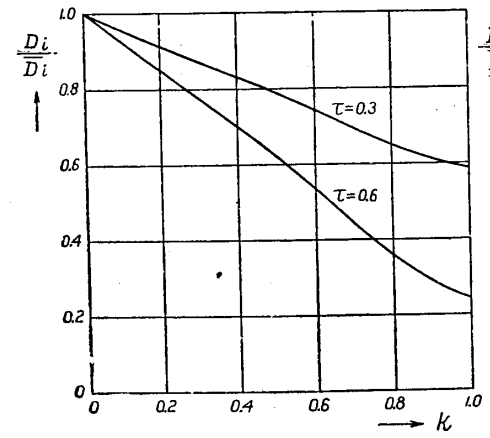

Fig. 32. The variation of the induced drag ratio $D_i/\bar{D}_i$ with the width of cut-out.

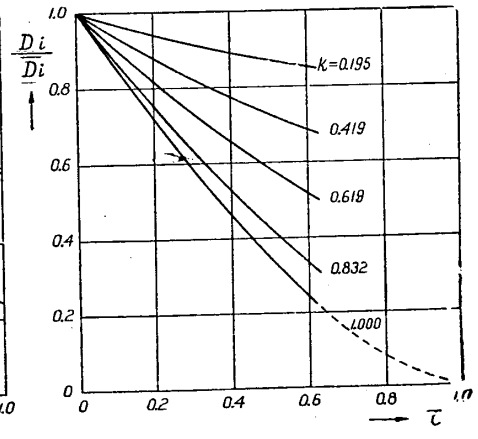

Fig. 33. The variation of the induced drag ratio $D_i/\bar{D}_i$ with the depth of cut-out.

Now, we shall compare the calculated results with the experimental results. The present calculation is based on the assumption that the axis of the aerofoil is a straight line parallel to the span, passing through the centre of pressure. Hence, it is doubtful whether the

present calculation can be applied to the case in which the axis of the aerofoil does not be a straight line as seen in the aerofoil with cut-out. For the purpose of discussing this the effects of removing the cut-out portion fore and aft on the characteristics of the aerofoil are measured with regard to the three aerofoils shown in Fig. 35. The measured results are shown in Figs. 36 and 37, showing that the

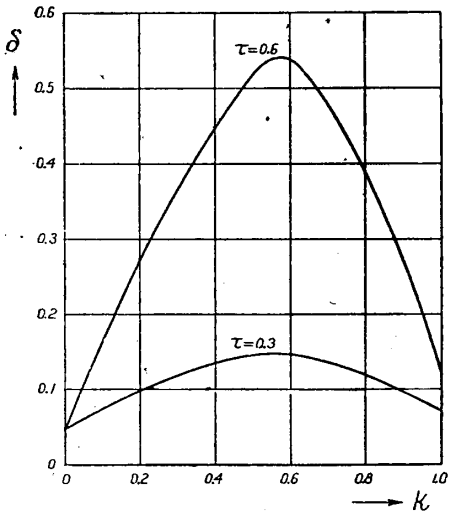

Fig. 34. The values of δ in the equation

$$c_{x_i} = \frac{c_z^2}{\pi\lambda}(1+\delta).$$

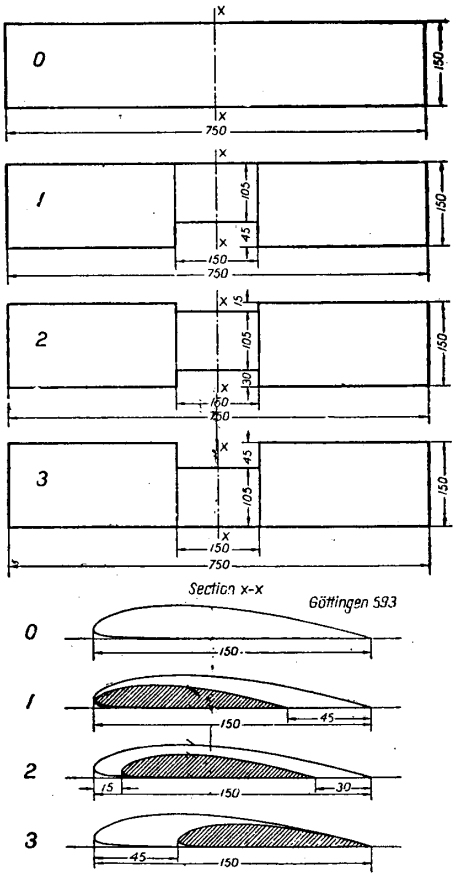

Fig. 35.

present calculation can be applied to all aerofoils tested as long as the angle of incidence is not too large. We shall compare the calculated result with the measured result with regard to the aerofoil 1 shown in Fig. 35. The lift coefficient, the induced drag coefficient and the profile drag coefficient of the aerofoil with cut-out are

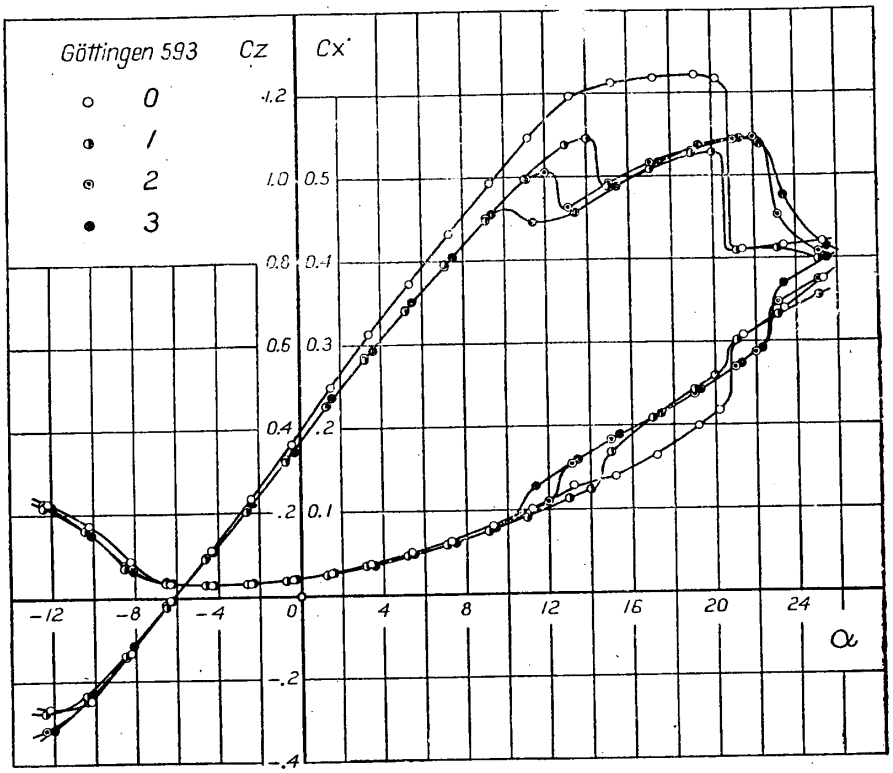

Fig. 36. The curves of the lift coefficient and the drag coefficient (referred to the area of the original aerofoil).

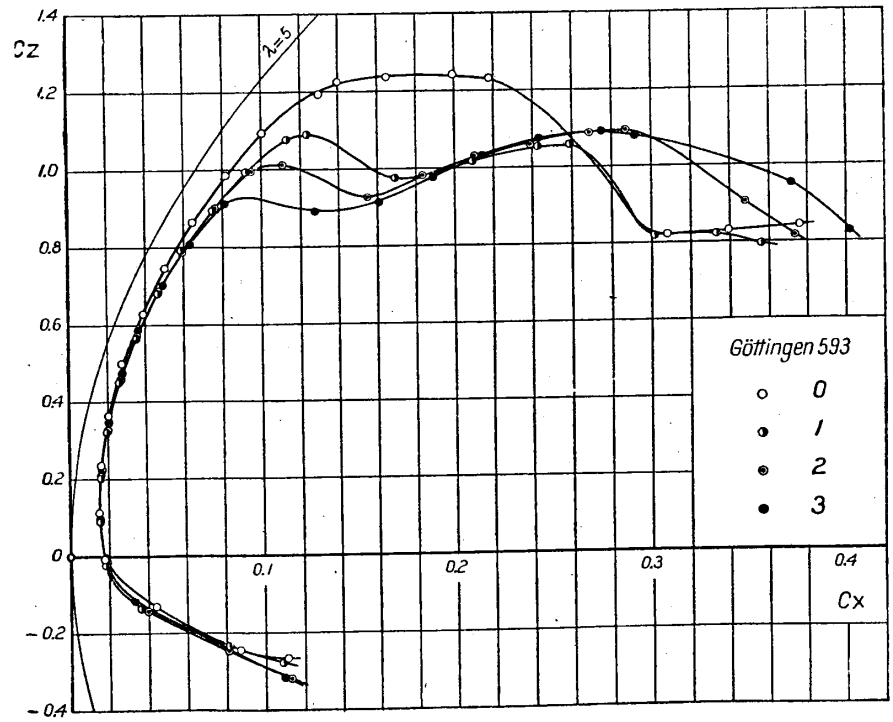

Fig. 37. The polar curves (referred to the area of the original aerofoil).

$$C_z = \bar{C}_z \mathfrak{L}\,, \quad C_{x_i} = \bar{C}_{x_i} \mathfrak{D}\,, \quad C_{x_p} = \bar{C}_{x_p}(1-k\tau)\,,$$

where the bar sign denotes the value for the original aerofoil. The drag coefficient of the aerofoil with cut-out becomes

$$C_x = \bar{C}_{x_i} \mathfrak{D} + \bar{C}_{x_p}(1-k\tau)\,.$$

The results obtained from the above equations with regard to the aerofoil with cut-out of $k = 0{\cdot}2$ and $\tau = 0{\cdot}3$ are compared with the experimental results in Fig. 38, showing that the agreement between the theory and the experiment is very satisfactory.

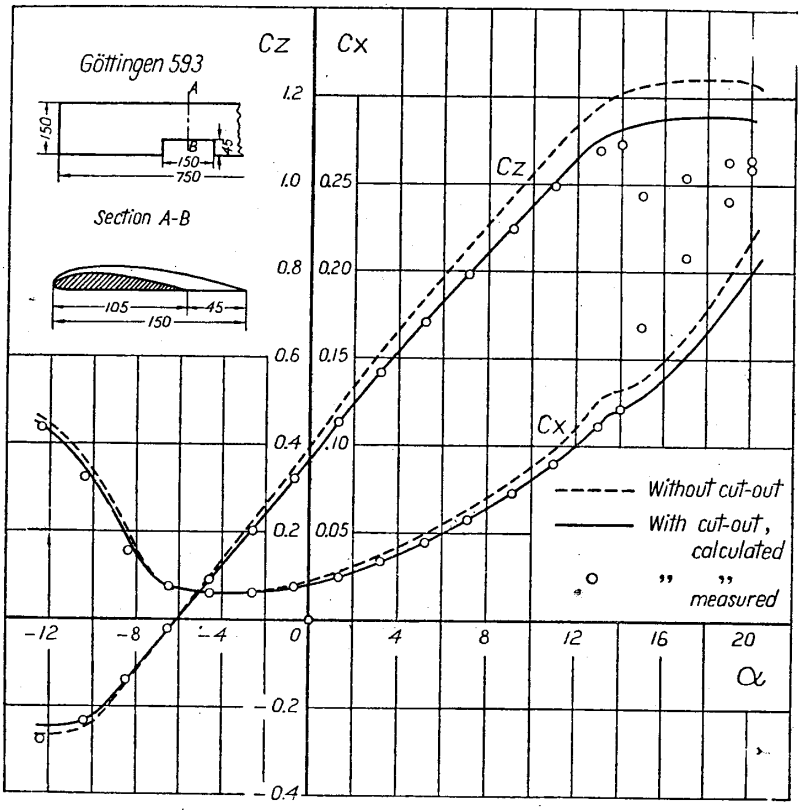

Fig. 38. The comparison of the calculated result with the experimental rescult.

It is interpreted from Fig. 26 that the stalling begins at first at the corner of the cut-out portion and it extends towards the wing centre and then the secondary stalling occurs near the centre of the tip

portion. For the purpose of confirming the theoretical consideration on the stalling the flow over the upper surface of the aerofoil 2 shown in Fig. 35 is observed by photographing the motion of the silk threads

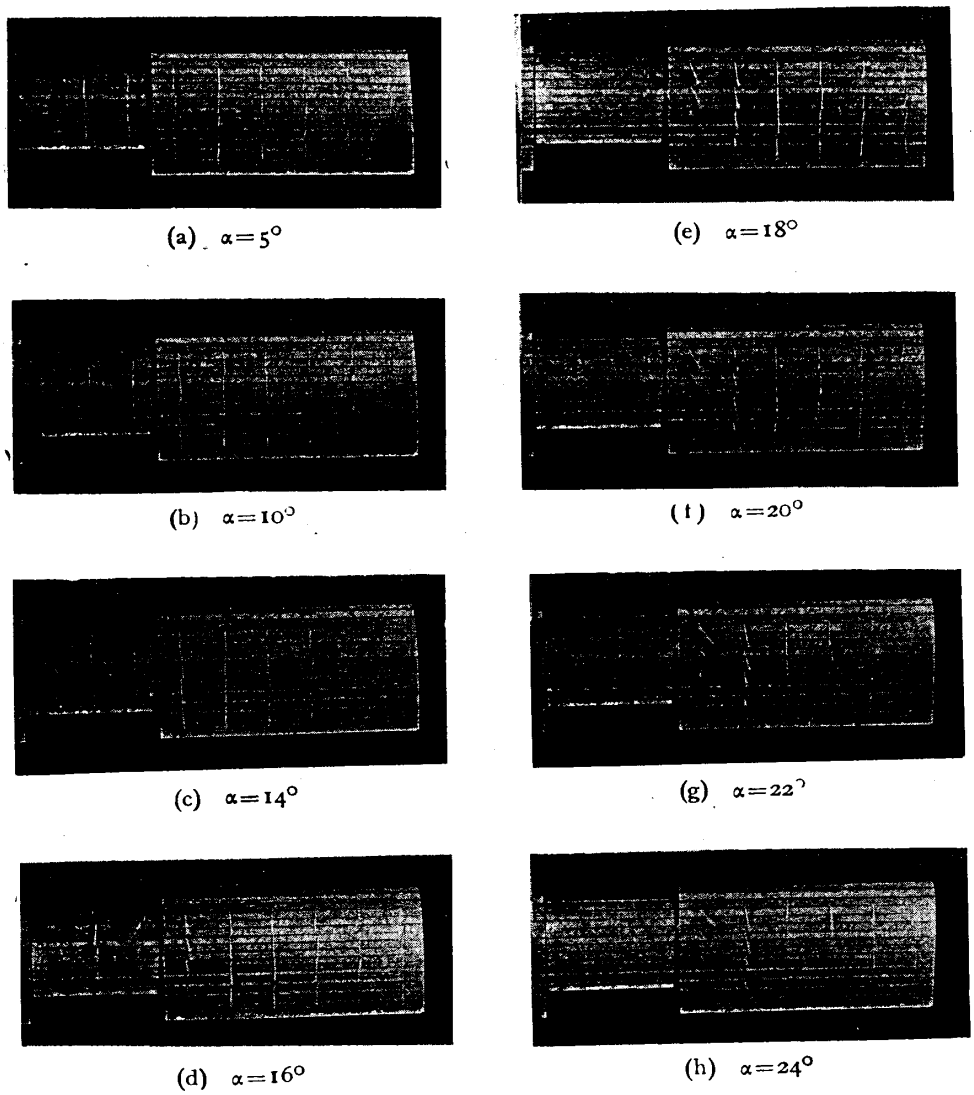

Fig. 39. The stalling of the aerofoil with cut-out.

set on the surface. The photographs are shown in Fig. 39. The theoretical consideration on the stalling is confirmed satisfactorily by the experiments.

§3.4. *The characteristics of the aerofoil with rectangular cut-out in which the geometrical angle of incidence is constant and* $\partial C_{z\infty}/\partial\alpha$ *and the chord length vary discontinuously along the span.*

We shall calculate the lift distribution of the aerofoil with rectangular cut-out in which the cut-out section is left just as the trailing edge is cut off as shown in Fig. 40. The calculations are carried out with regard to the cases in which the widths of cut-out are varied in $k = 0{\cdot}195$, $0{\cdot}419$, $0{\cdot}619$, $0{\cdot}832$ and $1{\cdot}000$ for the constant depth of cut-out of $\tau = 0{\cdot}3$, where the aspect ratio of the original aerofoil is 5. The coefficients C_{2n} and D_{2n} are determined to satisfy at twenty points $\theta = \pi/40$, $2\pi/40$, $\cdots$ $\pi/2$ the following conditions of the aerofoil shape:

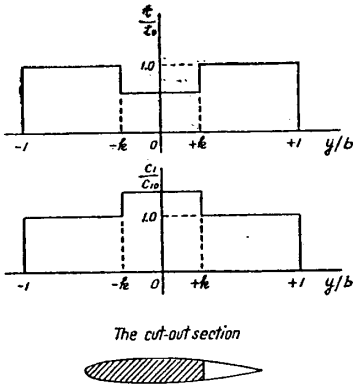

Fig. 40.

TABLE 7.

	$\tau=0$	$\tau=0{\cdot}3$				
	$k=0$	$k=\cdot195$	$k=\cdot419$	$k=\cdot619$	$k=\cdot832$	$k=\cdot1000$
A_1	+·9140	+·8797	+·8447	+·8162	+·7924	+·7837
A_3	+·1101	+·1314	+·1440	+·1398	+·1196	+·1057
A_5	+·0233	+·0081	+·0090	+·0245	+·0328	+·0243
A_7	+·0067	+·0171	+·0078	−·0016	+·0085	+·0073
A_9	+·0024	−·0043	+·0067	+·0040	+·0000	+·0027
A_{11}	+·0011	+·0055	−·0035	+·0043	−·0012	+·0012
A_{13}	+·0005	+·0037	+·0026	−·0014	+·0003	+·0006
A_{15}	+·0003	+·0017	+·0009	−·0010	+·0015	+·0003
A_{17}	+·c002	+·0009	−·0017	+·0018	+·0011	+·0002
A_{19}	+·0001	−·0011	+·0018	+·0004	−·0000	+·0001

$$\frac{t_{(y)}}{t_0} = 1\,, \qquad \frac{c_{1(y)}}{c_{10}} = 1 \qquad \text{for} \quad 0 \leqq \theta \leqq \theta_1\,,$$

$$\frac{t_{(y)}}{t_0} = 0{\cdot}7\,, \qquad \frac{c_{1(y)}}{c_{10}} = 1{\cdot}1674^{\dagger}$$

$$\text{for} \quad \theta_1 < \theta \leqq \frac{\pi}{2}\,,$$

where θ_1 is given by the relation $k = -\cos\theta_1$.

We thus determine the first ten coefficients $A_1, A_3, \cdots A_{19}$, which are tabulated in Table 7, and we get the distribution of circulation along the span as shown in Fig. 41.

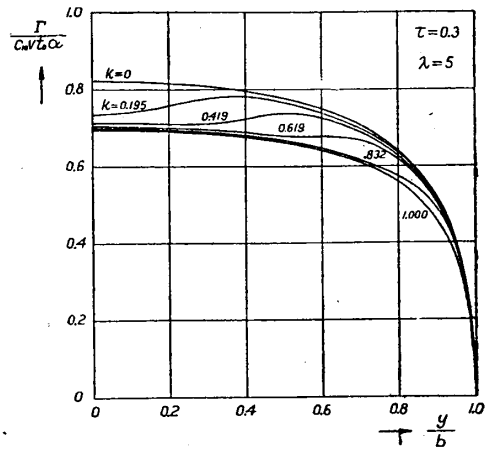

Fig. 41. The distribution of circulation along the span. (The depth of cu-out $\tau=0{\cdot}3$).

If we compare the distribution of circulation of the aerofoil, whose cut-out section is left just as the trailing edge is cut off, with that of

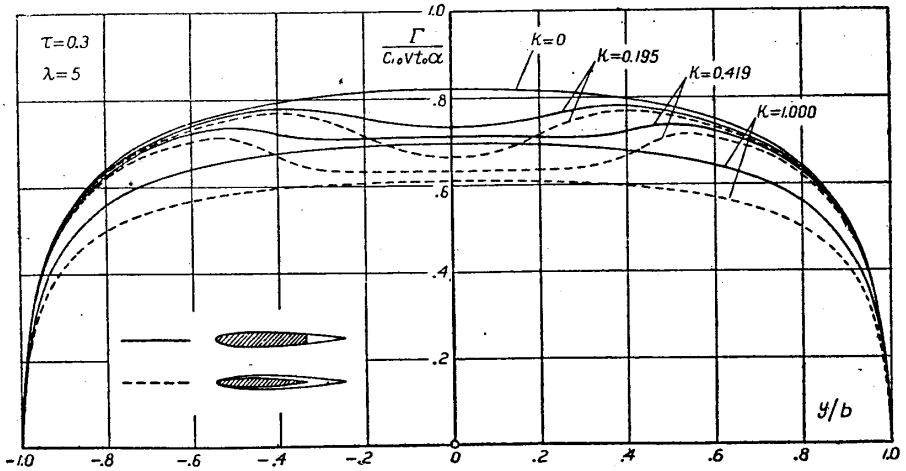

Fig. 42. The comparison of the distribution of circulation of the case in which $\partial c_{z\infty}/\partial\alpha$ increases at the out-cut portion with that of the case in which $\partial c_{z\infty}/\partial\alpha$ does not vary along the span.

†; This value is taken from Fig. 17.

the case studied in the preceding article, in which the value of $\partial C_{z\infty}/\partial a$ is constant along the span, then we know that the former has the greater lift as shown in Fig. 42.

The distributions of the induced velocity and the effective angle of incidence along the span are shown in Fig. 43, and the distribution of the induced drag along the span is shown in Fig. 44.

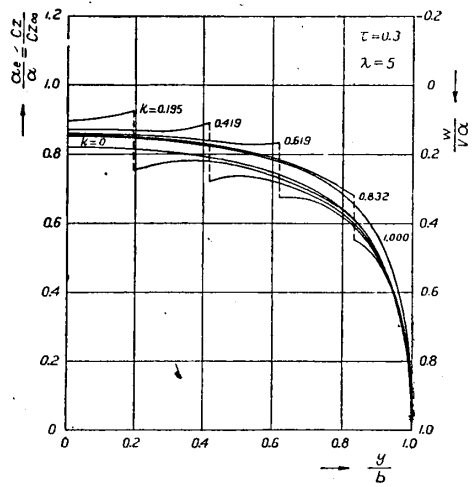

Fig. 43. The distributions of the induced velocity, the effective angle of incidence along the span.

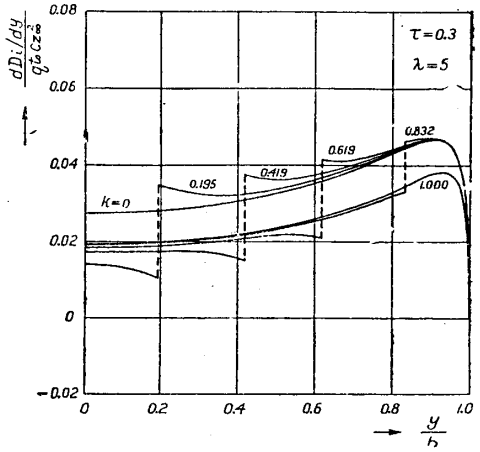

Fig. 44. The distribution of the induced drag along the span.

The ratio of the lift of the aerofoil with cut-out to that of the original aerofoil at the given angle of incidence is tabulated in Table 8

TABLE 8. Values of $\mathfrak{L}$, $\mathfrak{D}$, δ

	$\tau=0$ $k=0$	$\tau=0.3$				
		$k=.195$	$k=.419$	$k=.619$	$k=.832$	$k=1.000$
$\mathfrak{L}$	1.0000	.9625	.9241	.8930	.8669	.7345
$\mathfrak{D}$	1.0000	.9473	.8885	.8324	.7735	.7442
δ	.0473	.0710	.0894	.0932	.0778	.0601

and shown in Fig. 45. The ratio of the induced drag of the aerofoil with cut-out to that of the original aerofoil is shown in Table 8 and Fig. 46, and the values of δ in the equation of the induced drag coefficient are shown in Table 8 and Fig. 47.

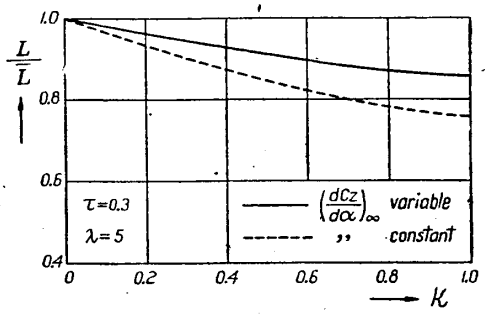

Fig. 45. The variation of the lift ratio $\mathfrak{L}$ with the width of out-out.

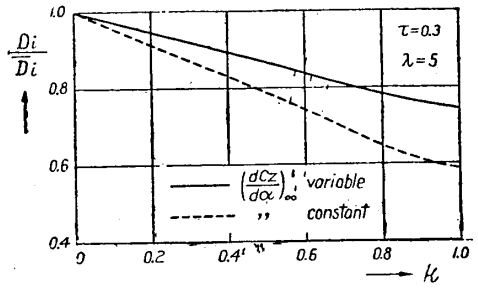

Fig. 46. The variation of the induced drag ratio $\mathfrak{D}$ with the width of cut-out.

Now, we shall compare the theoretical results with the experimental results. The experiment is carried out with regard to the 75 cm × 15 cm rectangular aerofoil of Göttingen 459 section. The lift coefficient and the induced drag coefficient of the aerofoil with cut-out at the given angle of incidence are calculated from the characteristics of the original aerofoil by the following equations

$$C_z = \bar{C}_z \mathfrak{L} , \quad C_{x_i} = \bar{C}_{x_i} \mathfrak{D} ,$$

and the profile drag coefficient of the aerofoil with cut-out becomes

$$C_{x_p} = \bar{C}_{x_p}(1-k)+C'_{x_p}k ,$$

where C'_{xp} is the profile drag coefficient of the aerofoil of $\tau = 0{\cdot}3$ and $k = 1{\cdot}0$. Hence, the drag coefficient of the aerofoil with cut-out becomes

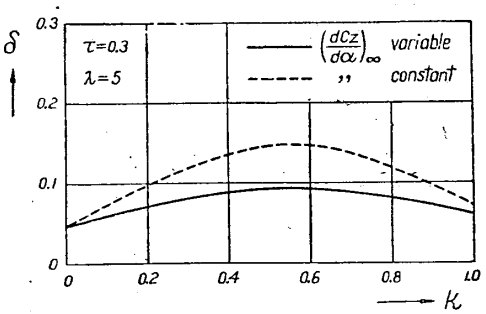

Fig. 47. The variation of the value of δ width of cut-out.

$$C_x = \bar{C}_{x_i}\mathfrak{D}+\bar{C}_{x_p}(1-k)+C'_{x_p}k .$$

The comparison of the calculated results with the experimental results (Reference 12) shows a good agreement between them as shown in Figs. 48 and 49.

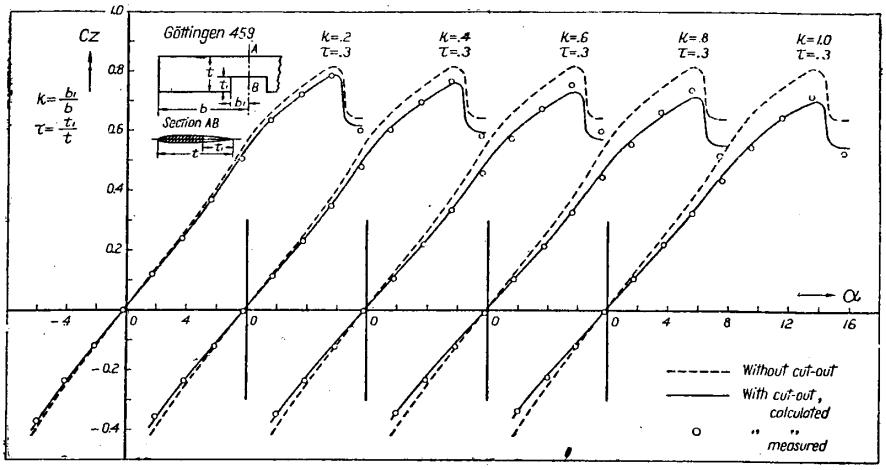

Fig. 48. The comparison of the calculation with the experiment with regard to the lift curve.

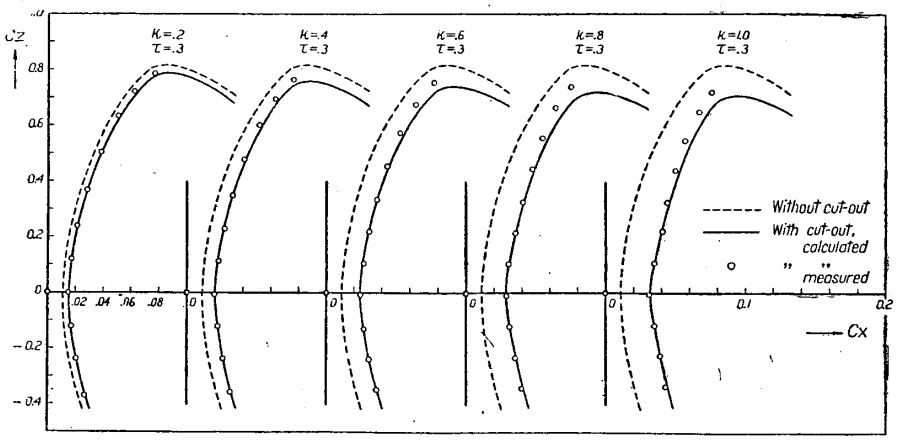

Fig. 49. The comparison of the calculation with the experiment with regard to the polar curve.

In conclusion the author wishes to acknowledge his best thanks to Prof. Dr. K. Wada for his cordinal guidance.

The Wind Tunnel Department,
The Aeronautical Research Institute,
Tokyo Imperial University, 1940.

References.

1. A. Betz u. E. Petersohn; Zur Theorie der Querruder. Z.a.M.M. 1928.
2. J. Edward; The integral calculus. Vol. 1, p. 196.
3. Ergehnisse der Aerodynamischen Versuchsanstalt zu Göttingen. Lief. I, III, IV.
4. Test of a thin low drag aerofoil, R.A.F. 25; R. & M. No. 915.

   F. B. Bradfield & A. S. Hartshorn: Test of three aerofoils suitable for high speed. R. & M. No. 943.

   F. B. Bradfield & A. S. Hartshorn; Test of four thick aerofoils R.A.F. 30, 31, 32 and 33. R. & M. No. 928.

   A. S. Hartshorn & H. Davis; Test of two aerofoils, R.A.F. 27 and R.A.F. 28. R. & M. No. 1027.
5. F. A. Louden; Collection of wind-tunnel data on commonly used wing sections. N.A.C.A. Tech, Rep. No. 331, 1929.
6. B. Ushakoff; Aerodynamic characteristics of Aerofoils, tested in the wind tunnel T—1 of the Central Aero-Hydrodynamical Institute. Trans. C.A.H.I. No. 193, 1935.
7. Service Technique de l'Aeronautique, Bulletin Technique, No. 12. 1923.
8. A Silverstein; Scale effect on Clark *Y* airfoil characteristics from N.A.C.A. Full-Scale wind-tunnel tests. N.A.C.A. Tech. Rep. No. 502, 1934.
9. C. B. Millikan & A. L. Klein; The effect of turbulence. Aircraft Engng. No. 54, 1933.
10. M. Lagally; Sitzungsberichte der Bayr. Akad. des Wiss., 1921.
11. I. Lotz; Berechnung der Auftriebsverteilung beliebig geformter Flügel. Z.F.M. 1931.
12. T. Okamoto; The Experimental Investigation of the Effects of a Cut-Out on the Wing Characteristics. Rep. Aero. Res. Inst. Tokyo Imp. Univ. No. 113, 1934.